Numerische Mathematik (2020) 145:973–1004
https://doi.org/10.1007/s00211-020-01129-9

Numerische Mathematik

H^1, $H(\mathrm{curl})$ and $H(\mathrm{div})$ conforming elements on polygon-based prisms and cones

Wenbin Chen[1] · **Yanqiu Wang**[2]

Received: 25 January 2019 / Revised: 5 September 2019 / Published online: 26 June 2020
© Springer-Verlag GmbH Germany, part of Springer Nature 2020

Abstract
The conation and extrusion techniques were proposed by Bossavit (Math Comput Simul 80:1567–1577, 2010) for constructing $(m+1)$-dimensional Whitney forms on prisms/cones from m-dimensional ones defined on the base shape. We combine the conation and extrusion techniques with the 2D polygonal $H(\mathrm{div})$ conforming finite element proposed by Chen and Wang (Math Comput 307:2053–2087, 2017), and construct the lowest-order H^1, $H(\mathrm{curl})$ and $H(\mathrm{div})$ conforming elements on polygon-based prisms and cones. The elements have optimal approximation rates. Despite of the relatively sophisticated theoretical analysis, the construction itself is easy to implement. As an example, we provide a 100-line Matlab code for evaluating the shape functions of H^1, $H(\mathrm{curl})$ and $H(\mathrm{div})$ conforming elements as well as their exterior derivatives on polygon-based cones. Note that all convex and some non-convex 3D polyhedra can be divided into polygon-based cones by connecting the vertices with a chosen interior point. Thus our construction also provides composite elements for all such polyhedra.

Mathematics Subject Classification 65N30

1 Introduction

In this paper, we aim at constructing lowest-order H^1, $H(\mathrm{curl})$ and $H(\mathrm{div})$ conforming elements on prisms and cones with polygonal bases. It has long been known [2,5,6,22,23] that the Whitney forms play an important role in such a construction. The original Whitney forms [35] were defined on simplices. But researchers have extended the idea

✉ Yanqiu Wang
yqwang@njnu.edu.cn

Wenbin Chen
wbchen@fudan.edu.cn

1 School of Mathematical Sciences and Shanghai Key Laboratory for Contemporary Applied Mathematics, Fudan University, Shanghai 200433, People's Republic of China

2 School of Mathematical Sciences, Nanjing Normal University, Nanjing, People's Republic of China

to hypercubes [26], triangular prisms [27], rectangular-based pyramids [22], and even some polytopes [8,9,20]. Constructing Whitney or Whitney-like forms on general 3D polyhedra is not easy. Among the works [8,9,20] mentioned above, the construction in [9] uses (discrete) harmonic functions and thus is expensive to compute; the one in [20] directly transplants the formula of simplicial Whitney forms to polytopes and results in too many redundant linearly-dependent basis functions; the authors of [8] propose a set of minimal degree forms but the forms work only on limited type of 3D polyhedra. Though, on 2D arbitrary convex polygons, the minimal degree Whitney-like forms given in [8] work quite well, which motivates the current work. In this paper, we will use the conation and extrusion techniques [7] to lift the Whitney-like forms in [8] from a 2D polygon to the 3D polygon-based prism/cone, and thus construct basis functions for H^1, $H(\text{curl})$ and $H(\text{div})$ conforming finite elements on the prism/cone.

In [7], Bossavit introduced the conation and extrusion techniques for constructing Whitney forms on triangles, rectangles, tetrahedra, rectangular boxes, triangular prisms, and pyramids, etc. The idea is to: (1) view rectangles, triangular prisms and rectangular boxes as "extrusion" of line segments, triangles and rectangles, respectively, so that Whitney forms on these shapes can be constructed by an "extrusion" technique from Whitney forms on corresponding base shapes; (2) similarly, view triangles, tetrahedra and pyramids as "conation" of line segments, triangles and rectangles, respectively, so that Whitney forms on them can be constructed by a "conation" technique. Moreover, as long as the Whitney forms on the base shape satisfy the discrete de Rham complex, it is guaranteed that the induced Whitney forms on the prisms/cones also satisfy the discrete de Rham complex.

Bossavit's theory was indeed developed for arbitrary base shapes and any dimensions, although in [7] it was only applied to triangular and rectangular base shapes. When applying the conation and extrusion techniques to general polygonal base shapes, there are still some non-trivial technical details that need to be clarified. The main contributions of this paper are: (1) we innovatively combine the conation and extrusion techniques with the Whitney forms on convex polygons [8] and thus construct practical lowest-degree H^1, $H(\text{curl})$ and $H(\text{div})$ conforming finite elements on polygon-based prisms and cones; (2) we prove that the new elements are conforming, derive optimal interpolation error estimates, and provide an efficient implementation.

We also mention a few other popular ways of defining H^1, $H(\text{curl})$ and $H(\text{div})$ finite elements on polytopes: the popular virtual element method (see the survey paper [3]) in which the basis functions are not explicitly known, the weak Galerkin method [32, 33] which uses weakly defined differential operators on discontinuous finite element spaces, and the hybrid high-order (HHO) method [10–12] which uses a nonconforming approach, etc. The list is far from complete, especially given that there is an increasing interest on such a topic. Some approaches, including those listed above, have fewer limitations on the mesh than the one proposed in this work.

The rest of the paper is organized as follows. A brief introduction to the reconstruction operator (for example the Whitney forms) is given in Sect. 2, together with a description of the Whitney forms on polygons defined in [8]. In Sect. 3, we introduce the idea of conation and extrusion proposed by Bossavit [7], and then apply it to polygon-based prisms and cones. In Sect. 4, the new elements are described and proved to be conforming. Implementation details and tricks will be presented in Sect. 5.

In Sect. 6, we derive optimal interpolation error estimates for the elements. Finally, numerical results will be given in Sect. 7.

For simplicity, we restrict out attention to convex base polygons. Though we point out that the idea of conation and extrusion can be readily extended to non-convex simply-connected base polygons, provided that there is a suitable set of Whitney forms defined on it.

2 The reconstruction operator

In recent years, researchers noticed that the process of constructing finite element spaces using given degrees of freedom can be viewed as a reconstruction operator, an inverse of the interpolation operator. A good overview and list of references can be found in the introduction of [4]. An early example of reconstruction is given by Whitney [35]. Therefore the reconstruction operator is also called a "Whitney map" in the literature.

For simplicity, we consider the local reconstruction operator on one single polytope K in the Euclidean space $\mathbb{R}^m$. A p-dimensional, $p = 0, 1, \ldots, m$, facet of K is called a p-cell. For example, vertices, edges, polygons and polyhedra are called p-cells, for $p = 0$, 1, 2, and 3, respectively. We view the p-cells as closed, i.e., each contains its boundary. The p-cells are also oriented, i.e., they are embedded into oriented p-manifolds. For example, each 0-cell (point) has a positive or negative sign, each 1-cell (edge) has a chosen positive direction, 2-cell (face) has a chosen positive side, and 3-cell (polyhedron) has a positive interior or exterior. Readers may find more about how to present the orientation of p-cells in [24]. Then, an m-dimensional polytope K can be viewed as a collection of p-cells, for $p = 0, 1, \ldots, m$. Denote by K_p the set of all p-cells in K and by N_P the cardinality of K_p.

Let $\Lambda^p(K)$ be the space of smooth differential p-forms on K. An exterior derivative d maps p-forms to $(p+1)$-forms. One may read more about differential forms and the exterior derivative in the books [1,18] or the survey paper [2]. On $K \subset \mathbb{R}^m$, one has the extended de Rham complex:

$$0 \longrightarrow \mathbb{R} \xrightarrow{\subset} \Lambda^0(K) \xrightarrow{\mathrm{d}} \Lambda^1(K) \xrightarrow{\mathrm{d}} \cdots \xrightarrow{\mathrm{d}} \Lambda^m(K) \longrightarrow 0.$$

The above complex is exact when K is contractable. On an m-manifold, all differential p-forms with $p > m$ are 0. Thus one only needs to consider p-forms for $0 \le p \le m$.

Each $w \in \Lambda^p(K)$ can be integrated on any oriented p-cell $\sigma \in K_p$, where the integration of a 0-form over a 0-cell is defined by evaluating the 0-form at the 0-cell (point) and then multiplying the value with the sign (orientation) of the 0-cell. Denote

$$\langle \sigma,\ w \rangle = \int_\sigma w.$$

Define a p-covector to be a vector in $\mathbb{R}^{N_p}$ whose ith entry is associated with the ith p-cell in K_p. Denote by $\mathcal{C}^p(K)$ the space of p-covectors. The local reconstruction operator $\mathcal{I}^p : \mathcal{C}^p(K) \to \Lambda^p(K)$ is defined to be a linear operator satisfying

$$\langle \sigma,\ \mathcal{I}^p(\boldsymbol{c})\rangle = [\boldsymbol{c}]_\sigma, \qquad \text{for all } \sigma \in K_p,\ \boldsymbol{c} \in \mathcal{C}^p(K),$$

where $[\boldsymbol{c}]_\sigma$ denotes the entry of $\boldsymbol{c}$ associated with the p-cell σ. In the finite element literature, the Whitney map [5,6,35] is probably one of the most well-known reconstruction operator and has been well-studied on simplices, hypercubes, pyramids, and prisms [7,21–23,26–28].

On a general polytope K, one may define the reconstruction operator by specifying the value of $\mathcal{I}^p$ over the canonical basis of $\mathcal{C}^p(K)$, i.e., specifying a set of p-forms $\{w_\sigma^p\}$ satisfying

$$\langle \sigma',\ w_\sigma^p\rangle = \begin{cases} 1 & \text{if } \sigma = \sigma' \\ 0 & \text{otherwise} \end{cases}, \tag{1}$$

for all $\sigma, \sigma' \in K_p$. Works in this direction [8,9,20] usually employ the generalized barycentric coordinates (GBCs) [14,15,17,25,29–31,34], and thus the resulting w_σ^p may not be as smooth as the polynomial-based Whitney forms on simplices. We shall introduce the Sobolev spaces of differential forms $H\Lambda^p(K)$, in which the forms and their exterior derivatives are both in L^2. One may find a rigorous definition of $H\Lambda^p(K)$ in [2]. Then the reconstruction $\mathcal{I}^p$ on general polytope K shall be considered as a linear map from $\mathcal{C}^p(K)$ to $H\Lambda^p(K)$. Nevertheless, since $\Lambda^p(K)$ is dense in $H\Lambda^p(K)$, some properties of differential forms will only be mentioned in $\Lambda^p(K)$ as they can be easily extended to $H\Lambda^p(K)$.

The range of $\mathcal{I}^p$ is then just

$$\mathcal{R}(\mathcal{I}^p) = span\{w_\sigma^p,\ \text{for } \sigma \in K_p\},$$

which is a finite dimensional subspace of $H\Lambda^p(K)$. From (1), it is not hard to see that w_σ^ps, for $\sigma \in K_p$, form a basis for $\mathcal{R}(\mathcal{I}^p)$. Indeed w_σ^ps are also the key to defining finite element bases on K. In this sense, they play the same role as Whitney forms in the definition of simplicial finite elements. Thus, we will call w_σ^p *Whitney forms*, although their construction may be different from the traditional Whitney forms given in [35].

Remark 2.1 When the p-cells in K_p are indexed by $i = 1, \ldots, N_p$, we conveniently denote w_σ^p, for $\sigma \in K_p$, by w_i^p, for $i = 1, \ldots, N_p$.

For reader's convenience, we mention a few general rules about the computation of differential forms, while more details can be found in [1,2,18]. The exterior (wedge) product of two differential forms $w \in \Lambda^p(K)$ and $\eta \in \Lambda^q(K)$ is a $(p+q)$-form and satisfies

$$w \wedge \eta = (-1)^{pq}\, \eta \wedge w.$$

The 0-form is special since it can be viewed as a scalar function. Its wedge product with any p-form can thus be viewed as plain multiplication. Therefore we often write

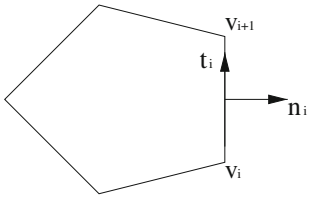

Fig. 1 Illustration of the unit outward normal vector $\boldsymbol{n}_i$ and the unit tangent vector $\boldsymbol{t}_i$

the wedge product of a 0-form w with a p-form η as their product, i.e., $w \wedge \eta = w\,\eta$. The exterior derivative of the wedge product satisfies:

$$\mathrm{d}(w \wedge \eta) = \mathrm{d}w \wedge \eta + (-1)^j w \wedge \mathrm{d}\eta, \qquad \text{for } w \in \Lambda^j(K) \text{ and } \eta \in \Lambda^k(K).$$

From the de Rham complex, one gets $\mathrm{d}^2 = 0$.

2.1 A 2D reconstruction operator on convex polygons

Here we briefly describe a reconstruction operator defined on convex polygons, which is built upon the generalized barycentric coordinates (GBCs) [14,15,17,25,29–31,34] and the H(div)-conforming polygonal element proposed in [8].

Let K be a convex polygon lying on the xy-plane. Denote by $\boldsymbol{v}_i$, $1 \le i \le n$, the vertices of K ordered counter-clockwise. Denote by e_i the edge from $\boldsymbol{v}_i$ to $\boldsymbol{v}_{i+1}$, where we conveniently set $\boldsymbol{v}_j = \boldsymbol{v}_{j\,(\mathrm{mod}\,n)}$ when the subscript j is not in the range of $\{1, \ldots, n\}$. We view K_0 as the collection of $\boldsymbol{v}_i$s, each assigned a positive sign; K_1 as the collection of e_is, each oriented counter-clockwise; and K_2 containing just the polygon K with the same orientation as the xy axes.

The generalized barycentric coordinates (GBCs) on K are defined as functions λ_i, for $i = 1, \ldots, n$, that satisfy

1. (Non-negativity) All λ_i, for $1 \le i \le n$, have non-negative value on K;
2. (Linear precision) For any linear function $L(\boldsymbol{x})$ defined on K, one has

$$L(\boldsymbol{x}) = \sum_{i=1}^{n} L(\boldsymbol{v}_i)\lambda_i(\boldsymbol{x}), \qquad \text{for all } \boldsymbol{x} \in K.$$

The linear precision property is indeed equivalent to the combination of the unit decomposition and the Lagrange properties: for all $\boldsymbol{x} \in K$,

$$\sum_{i=1}^{n} \lambda_i(\boldsymbol{x}) = 1, \qquad \sum_{i=1}^{n} \lambda_i(\boldsymbol{x})\,\boldsymbol{v}_i = \boldsymbol{x}. \tag{2}$$

The linear precision property also suggests that $span\{\lambda_i,\ 1 \le i \le n\}$ contains the space of all linear polynomials, which is essential to the interpolation error analysis.

Denote by $\boldsymbol{n}_i$ and $\boldsymbol{t}_i$ the unit outward normal, with respect to K, and the unit tangent vector on the edge e_i. An illustration is given in Fig. 1. Choose an arbitrary point $\boldsymbol{x}_*$

inside the polygon K, and denote by K_i the triangle with base e_i and apex $\boldsymbol{x}_*$. Denote by d_i the distance from $\boldsymbol{x}_*$ to e_i. Let $|e_i|$, $|K_i|$ and $|K|$ be the length of e_i, the area of K_i and K, respectively. We use the standard notation $L^p(K)$, $W^{s,p}(K)$, $H^s(K)$ and $H(\mathrm{div}, K)$, with $s \in \mathbb{R}$ and $1 \leq p \leq \infty$ for different type of Sobolev spaces, equipped with corresponding norms. For simplicity, denote by $\|\cdot\|_K$ and $\|\cdot\|_{e_i}$ the L^2 norm on K and e_i respectively, while by $\|\cdot\|_{1,K}$ the H^1 norm on K. Finally, denote by h_K the diameter of K.

For $1 \leq i, l \leq n$, define

$$b_{i,l} = \delta_{il}|e_l| - |e_i|\frac{|K_l|}{|K|},$$

where δ_{il} is the Kronecker Delta. The above notation can be extended to indices not in $\{1, \ldots, n\}$ using modular arithmetic. It has been proven in [8] that:

Lemma 2.2 *For each $1 \leq i \leq n$, define $\boldsymbol{q}_i = c_{i,0}(\boldsymbol{x} - \boldsymbol{x}_*) + \sum_{k=1}^{n} c_{i,k}\nabla^{\perp}\lambda_k$, where $c_{i,0} = \frac{|e_i|}{2|K|}$, $c_{i,k} = -\frac{1}{n}\sum_{l=1}^{n-1} l\, b_{i,k+l}$ and $\nabla^{\perp} = (-\partial_y, \partial_x)^t$. Then, one has $\boldsymbol{q}_i \cdot \boldsymbol{n}_j|_{e_j} \equiv \delta_{ij}$ for all $1 \leq j \leq n$.*

Using the above lemma, we are able to write the Whitney forms on K as follows:

- The 0-forms w_i^0, for $i = 1, \ldots, n$, are defined by

$$w_i^0 = \lambda_i,$$

  which satisfies $w_i^0(\boldsymbol{v}_j) = \delta_{ij}$.
- The 1-forms w_i^1, for $i = 1, \ldots, n$, are defined by

$$w_i^1 = \frac{-[\boldsymbol{q}_i]_2}{|e_i|}\mathrm{d}x + \frac{[\boldsymbol{q}_i]_1}{|e_i|}\mathrm{d}y, \tag{3}$$

  where $[\boldsymbol{q}_i]_1$ and $[\boldsymbol{q}_i]_2$ are the two components of the vector $\boldsymbol{q}_i$. By Lemma 2.2, one has $\int_{e_i} w_i^1 = \delta_{ij}$. Here we mention again that the 1-cells (edges) of K are oriented counter-clockwise.
- There is only one 2-form w_1^2, which is defined by

$$w_1^2 = \frac{1}{|K|}\mathrm{d}x \wedge \mathrm{d}y,$$

  and satisfies $\int_K w_1^2 = 1$.

The Whitney forms span $\mathcal{R}(\mathcal{I}^p)$, which for convenience is also denoted by $M^p(K)$, i.e.,

$$M^p(K) \triangleq \mathcal{R}(\mathcal{I}^p) = span\{w_i^p, \text{ for } i = 1, \ldots, N_p\},$$

where $N_0 = N_1 = n$ and $N_2 = 1$. It has been proven in [8] that $M^p(K)$ satisfy the following exact discrete de Rham complex:

$$0 \longrightarrow \mathbb{R} \xrightarrow{\subset} M^0(K) \xrightarrow{\mathrm{d}} M^1(K) \xrightarrow{\mathrm{d}} M^2(K) \longrightarrow 0.$$

By the property of GBC, we know that the space $M^0(K)$ contains all linear functions. In [8], it has been proved that $M^1(K)$ also contains a space related to the lowest-order triangular Raviart–Thomas finite element space [28]:

Lemma 2.3 *The space $M^1(K)$ contains*

$$\{f\,\mathrm{d}x + g\,\mathrm{d}y,\ \textit{for all}\ \begin{bmatrix} g \\ -f \end{bmatrix} = c_0\boldsymbol{x} + \boldsymbol{c}\ \textit{where}\ \boldsymbol{c} = \begin{bmatrix} c_1 \\ c_2 \end{bmatrix}\ \textit{and}\ c_0, c_1, c_2 \in \mathbb{R}\}.$$

Next, we carefully examine the basis $\{w_i^1\}$ in the case when K is a triangle or a rectangle, as it plays an important role in our 3D reconstruction.

Lemma 2.4 *When K is a triangle, $\boldsymbol{q}_i$s are identical to the Whitney basis functions of the lowest-order Raviart–Thomas (RT_0) element on K. When K is a rectangle and the generalized barycentric coordinate is chosen such that*

$$\lambda_i = \textit{the Lagrangian basis on vertex } \boldsymbol{v}_i \textit{ for } Q_1(K), \tag{4}$$

where $Q_1(K)$ denotes the space of bilinear polynomials on K, again $\boldsymbol{q}_i$s are identical to the Whitney basis functions of the lowest-order RT element on K.

Proof When K is a triangle, all GBCs on K are identical to the traditional triangular barycentric coordinates. From Lemma 2.2 one can easily compute that $\boldsymbol{q}_i$s lie in RT_0. By unisolvency, they must be identical to the RT_0 Whitney basis functions. The case when K is a rectangle is a little complicated, since there exist infinitely many GBCs on K. However, as long as one chooses a GBC satisfying (4), an elementary calculation shows that $\boldsymbol{q}_i$s lie in RT_0. Again they must be identical to the RT_0 Whitney basis functions. □

Remark 2.5 There are more than one GBCs satisfying (4), for example, the harmonic GBC [25] and the Wachspress GBC [30]. But there are GBCs, for example the piecewise-linear GBC, that do not satisfy (4).

Remark 2.6 Condition (4) can be weakened to

$$span\{\lambda_i,\ 1 \le i \le 4\} = Q_1(K),$$

and the result in Lemma 2.4 still holds.

Remark 2.7 On triangles, w_i^ps are identical to the traditional simplicial Whitney p-forms defined in [35]. Using the notation introduced by Arnold et. al. [2], one has $M^p(K) = \mathcal{P}_1^- \Lambda^p$ on a triangle K, for $p = 0, 1, 2$. Similarly, when K is a rectangle and the GBC satisfies (4), one has $M^p(K) = \mathcal{Q}_1^- \Lambda^p$.

Remark 2.8 The definition of w_i^p can be extended to non-convex polygons as long as one has well-defined GBCs on the polygon. In this paper, we restrict our attention on convex polygons because there are more GBCs available on convex ones, and the theoretical analysis is also more well-developed comparing to GBCs on nonconvex polygons.

The reconstruction on polygon $K \in \mathbb{R}^2$ can be easily generalized to any oriented planar polygon $F \in \mathbb{R}^3$, i.e., F lies on a plane, as long as one chooses a local Cartesian coordinate system for F that is compatible with its orientation. We use $\{w_{F,i}^p\}$, for $p = 0, 1, 2$, to denote the Whitney forms on F and $M^p(F)$ to denote the space spanned by the Whitney p-forms.

To simplify the notation, we also introduce spaces of Whitney p-forms on a 0-cell $\boldsymbol{v}$ as

$$\begin{aligned} M^0(\boldsymbol{v}) &= \mathbb{R}, \\ M^p(\boldsymbol{v}) &= \{0\} \qquad \text{for } p \geq 1, \end{aligned}$$

and on a 1-cell e parametrized by $0 \leq t \leq 1$ as

$$\begin{aligned} M^0(e) &= \{\text{all linear functions on } e\}, \\ M^1(e) &= \{c\,\mathrm{d}t, \text{ for all } c \in \mathbb{R}\} = span\{\mathrm{d}t\}, \\ M^p(e) &= \{0\} \qquad \text{for } p \geq 2. \end{aligned}$$

3 Conation and extrusion

The idea of using conation or extrusion to construct higher dimensional Whitney forms from lower dimensional ones was introduced by Bossavit in [7]. In both processes, a base polytope is given in $\mathbb{R}^m$. The base polytope is embedded into a hyperplane in $\mathbb{R}^{m+1}$. Then, one can generate a cone in $\mathbb{R}^{m+1}$ by connecting points in the base polytope to an apex outside the hyperplane, or generate a prism in $\mathbb{R}^{m+1}$ by moving the base polytope along the normal direction of the hyperplane. Bossavit named the former "conation" and the latter "extrusion", and developed systematic formulae to lift the Whitney map from the base polytope to the higher-dimensional cone/prism. In this section, we shall briefly introduce Bossavit's work.

Since there are two polytopes involved in the process, an m-dimensional base polytope and an $(m+1)$-dimensional cone/prism, we shall name the base polytope $\underset{\sim}{K}$ and the cone/prism K. It is convenient to add a tilde as under-accent to every variable/function/form/operator associated with the base polytope $\underset{\sim}{K}$, in order to distinguish it from those defined on K. For example, a point in $\underset{\sim}{K}$ is denoted by $\underset{\sim}{\boldsymbol{x}} = (\underset{\sim}{x}_1, \underset{\sim}{x}_2, \ldots, \underset{\sim}{x}_m)^t$ where $(\underset{\sim}{x}_i)_{i=1}^m$ denotes a Cartesian coordinate system on $\underset{\sim}{K}$. A set of Whitney p-forms on $\underset{\sim}{K}$ is then denoted by $\{\underset{\sim}{w}_i^p\}_{1 \leq i \leq \underset{\sim}{N}_p}$, where $\underset{\sim}{N}_p$ is the cardinality of $\underset{\sim}{K}_p$.

Embed $\underset{\sim}{K}$ into $\mathbb{R}^{m+1}$, equipped with a Cartesian coordinate system $(x_i)_{i=1}^{m+1}$, so that the $\underset{\sim}{x}_1\underset{\sim}{x}_2 \ldots \underset{\sim}{x}_m$-coordinate coincides with the $x_1 x_2 \ldots x_m$-hyperplane, i.e., $x_{m+1} = 0$. Then we define K by either one of the following processes:

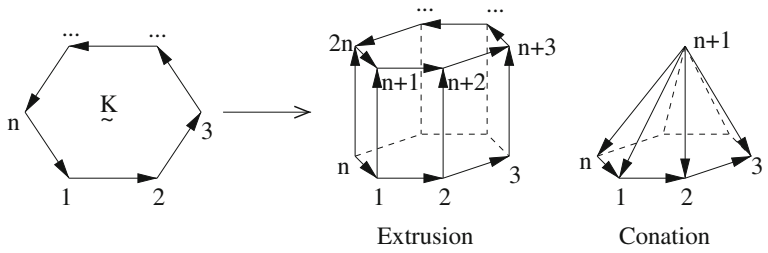

Fig. 2 Illustration of conation and extrusion from a base polygon with n vertices. The arabic numbers denote the indices of vertices, and the edge orientations are shown by arrows

Extrusion K is a prism with base $\underset{\sim}{K}$ and height θ, defined by

$$K = \left\{ ext(\underset{\sim}{x}, z) \triangleq \begin{bmatrix} \underset{\sim}{x} \\ \theta z \end{bmatrix} \text{ for all } \underset{\sim}{x} \in \underset{\sim}{K},\ 0 \le z \le 1 \right\};$$

Conation K is a cone with base $\underset{\sim}{K}$ and apex $(0, \ldots, 0, \theta)^t$, defined by

$$K = \left\{ con(\underset{\sim}{x}, z) \triangleq z \begin{bmatrix} \mathbf{0} \\ \theta \end{bmatrix} + (1 - z) \begin{bmatrix} \underset{\sim}{x} \\ 0 \end{bmatrix} \text{ for all } \underset{\sim}{x} \in \underset{\sim}{K},\ 0 \le z \le 1 \right\}.$$

Since we will study Whitney forms on K, it is important to specify the numbering and orientation of p-cells in K. For simplicity, we only describe the case when K is 3-dimensional. Let $\underset{\sim}{K}$ be a 2D polygon with n vertices, and let the p-cells of $\underset{\sim}{K}$ be ordered and oriented as shown in Fig. 2. Then the p-cells of K are defined by:

Numbering and orientation of p-cells for extrusion from 2D to 3D

- There are $2n$ vertices, in which
  - no. $1, \ldots, n$ are bottom vertices that come from the vertices of $\underset{\sim}{K}$;
  - no. $n+1, \ldots, 2n$ are top vertices such that the $(n+i)$th vertex is right above the ith vertex, for $i = 1, \ldots, n$.

  All 0-cells have positive orientation (sign).
- There are $3n$ edges, in which
  - no. $1, \ldots, n$ are bottom edges with the same order and orientation as in $\underset{\sim}{K}$;
  - no. $n+1, \ldots, 2n$ are top edges such that the $(n+i)$th edge is right above and with the same orientation of the ith edge, for $i = 1, \ldots, n$;
  - no. $2n+1, \ldots, 3n$ are side edges, each pointing from the ith vertex to the $(n+i)$th vertex, for $i = 1, \ldots, n$.
- There are $n+2$ faces, in which
  - no. 1 is the bottom face, facing upward;
  - no. 2 is the top face, facing upward;
  - no. $2+1, \ldots, 2+n$ are side faces facing outward, each formed by the ith and the $(n+i)$th edges, for $i = 1, \ldots, n$.

Numbering and orientation of p-cells for conation from 2D to 3D

- There are $n+1$ vertices, in which
  - no. $1, \ldots, n$ are bottom vertices that come from the vertices of $\underset{\sim}{K}$;
  - no. $n+1$ is the apex of the cone.

  All 0-cells have positive orientation (sign).
- There are $2n$ edges, in which
  - no. $1, \ldots, n$ are bottom edges with the same order and orientation as in $\underset{\sim}{K}$;
  - no. $n+1, \ldots, 2n$ are side edges, each pointing from the apex to the ith vertex, for $i = 1, \ldots, n$.
- There are $n+1$ faces, in which
  - no. 1 is the bottom face, facing upward;
  - no. $2, \ldots, n+1$ are side faces facing outward, each connected to the ith edge, for $i = 1, \ldots, n$.

The definition of conation/extrusion naturally induces a "projection" from K onto $\underset{\sim}{K}$: for point $\boldsymbol{x} = ext(\underset{\sim}{\boldsymbol{x}}, \underset{\sim}{z})$ or $\boldsymbol{x} = con(\underset{\sim}{\boldsymbol{x}}, \underset{\sim}{z})$, define

$$\pi(\boldsymbol{x}) = \underset{\sim}{\boldsymbol{x}}.$$

Remark 3.1 The projection π is well-defined on K except for the apex when K is a cone. This does not matter since we will show later that forms/functions defined using π can be extended continuously to the boundary of K. For simplicity of the notation, we temporarily consider K as $K \backslash \{apex\}$, i.e., $\boldsymbol{x} \in K$ actually means that $\boldsymbol{x}$ being any point in K except for the apex.

Remark 3.2 A point $\boldsymbol{x} = (x_1, x_2, \ldots, x_{m+1}) \in K$ can also be expressed in the coordinate $(\underset{\sim}{x}_1, \ldots, \underset{\sim}{x}_m, \underset{\sim}{z})$, with $\boldsymbol{x} = ext(\underset{\sim}{\boldsymbol{x}}, \underset{\sim}{z})$ or $\boldsymbol{x} = con(\underset{\sim}{\boldsymbol{x}}, \underset{\sim}{z})$ defining a coordinate transformation from $(\underset{\sim}{x}_1, \ldots, \underset{\sim}{x}_m, \underset{\sim}{z})$ to $(x_1, x_2, \ldots, x_{m+1})$. Note that $(x_1, x_2, \ldots, x_{m+1})$ is the usual Cartesian coordinate while $(\underset{\sim}{x}_1, \ldots, \underset{\sim}{x}_m, \underset{\sim}{z})$ is not even an orthogonal coordinate system in the case of conation. We call $(\underset{\sim}{x}_1, \ldots, \underset{\sim}{x}_m, \underset{\sim}{z})$ a "scaled" coordinate for point $\boldsymbol{x}$. For a function $\underset{\sim}{f}(\underset{\sim}{\boldsymbol{x}})$ defined on $\underset{\sim}{K}$, the function $\underset{\sim}{f} \circ \pi$ is defined on K. When considered in the scaled coordinate, $\underset{\sim}{f} \circ \pi$ has exactly the same expression as $\underset{\sim}{f}$. This will greatly simplify the calculation of finite element basis functions later.

In the sense of Remark 3.1, the projection π is a smooth map from K to $\underset{\sim}{K}$. It is standard to define a pushforward $\pi_* : T_{\boldsymbol{x}} K \to T_{\underset{\sim}{\boldsymbol{x}}} \underset{\sim}{K}$ for all $\boldsymbol{x} \in K$, where $T_{\boldsymbol{x}} K$ is the tangent space of K at point $\boldsymbol{x}$ and $T_{\underset{\sim}{\boldsymbol{x}}} \underset{\sim}{K}$ is the tangent space of $\underset{\sim}{K}$ at point $\underset{\sim}{\boldsymbol{x}} = \pi(\boldsymbol{x})$. By definition, π_* maps a derivation (or a tangent vector) $D \in T_{\boldsymbol{x}} K$ to a derivation $\pi_* D \in T_{\underset{\sim}{\boldsymbol{x}}} \underset{\sim}{K}$ satisfying

$$(\pi_* D) \underset{\sim}{f}\big|_{\underset{\sim}{\boldsymbol{x}}} = D(\underset{\sim}{f} \circ \pi)\big|_{\boldsymbol{x}} \qquad \text{for all } \underset{\sim}{f} \in C^\infty(\underset{\sim}{K}),$$

at each point $\boldsymbol{x} \in K$. It is also standard to define the pullback $\pi^* : \Lambda^p(\underset{\sim}{K}) \to \Lambda^p(K)$ of differential forms for $0 \le p \le m$ by

$$(\pi^* \underset{\sim}{w})(D_1, \ldots, D_p)\big|_{\boldsymbol{x}} = \underset{\sim}{w}(\pi_* D_1, \ldots, \pi_* D_p)\big|_{\underset{\sim}{x}} \quad \text{for all } \underset{\sim}{w} \in \Lambda^p(\underset{\sim}{K}),\ D_i \in T_{\boldsymbol{x}} K,$$

at each point $\boldsymbol{x} \in K$. Readers may refer to [1,18] for definitions of tangent/cotangent space, derivation/tangent vector, and pushforward/pullback. Here we shall mention that the pullback is compatible with both the exterior (wedge) product and the exterior derivative, i.e.,

$$\begin{aligned} \pi^*(\underset{\sim}{w}_1 \wedge \underset{\sim}{w}_2) &= \pi^*(\underset{\sim}{w}_1) \wedge \pi^*(\underset{\sim}{w}_2), && \text{for all } \underset{\sim}{w}_1 \in \Lambda^p(\underset{\sim}{K}),\ \underset{\sim}{w}_2 \in \Lambda^q(\underset{\sim}{K}), \\ \pi^*(\mathrm{d}\underset{\sim}{w}) &= \mathrm{d}(\pi^* \underset{\sim}{w}), && \text{for all } \underset{\sim}{w} \in \Lambda^p(\underset{\sim}{K}). \end{aligned} \tag{5}$$

In the case of conation we also denote

$$\Pi^* \underset{\sim}{w} = (1 - \underset{\sim}{z})^p \pi^* \underset{\sim}{w} \qquad \text{for } \underset{\sim}{w} \in \Lambda^p(\underset{\sim}{K}).$$

Here the superscript in $(1 - \underset{\sim}{z})^p$ means 'pth power'. It can be easily distinguished from the notation such as w_i^p in which p denotes p-forms, since $1 - \underset{\sim}{z}$ is obviously a 0-form (scalar function). Therefore we use both notations without special mentioning.

In [7], Bossavit gave the formula for constructing Whitney p-forms on K by using Whitney forms on $\underset{\sim}{K}$. Here we present Bossavit's construction. Suppose the numbering and the orientation of p-cells in $\underset{\sim}{K}$ and K are as described before. Given a set of Whitney p-forms $\{\underset{\sim}{w}_i^p\}$ on $\underset{\sim}{K}$, then one can define the Whitney p-forms $\{w_i^p\}$ on K as follows:

Extrusion

The total number of 0-forms is $2\underset{\sim}{N}_0$, each associated with

- bottom 0-cell: $w_i^0 = (1 - \underset{\sim}{z})\, \pi^* \underset{\sim}{w}_i^0$ for $i = 1, \ldots, \underset{\sim}{N}_0$;
- top 0-cell: $w_{\underset{\sim}{N}_0 + i}^0 = \underset{\sim}{z}\, \pi^* \underset{\sim}{w}_i^0$ for $i = 1, \ldots, \underset{\sim}{N}_0$.

The total number of p-forms, for $p \geq 1$, is $2\underset{\sim}{N}_p + \underset{\sim}{N}_{p-1}$, each associated with

- bottom p-cell: $w_i^p = (1 - \underset{\sim}{z})\, \pi^* \underset{\sim}{w}_i^p$ for $i = 1, \ldots, \underset{\sim}{N}_p$;
- top p-cell: $w_{\underset{\sim}{N}_p + i}^p = \underset{\sim}{z}\, \pi^* \underset{\sim}{w}_i^p$ for $i = 1, \ldots, \underset{\sim}{N}_p$;
- side p-cell: $w_{2\underset{\sim}{N}_p + i}^p = \pi^* \underset{\sim}{w}_i^{p-1} \wedge \mathrm{d}\underset{\sim}{z}$ for $i = 1, \ldots, \underset{\sim}{N}_{p-1}$.

Conation

The total number of 0-forms is $\underset{\sim}{N}_0 + 1$, each associated with

- bottom 0-cell: $w_i^0 = (1 - \underset{\sim}{z})\, \Pi^* \underset{\sim}{w}_i^0$ for $i = 1, \ldots, \underset{\sim}{N}_0$;
- top 0-cell: $w_{\underset{\sim}{N}_0 + 1}^0 = \underset{\sim}{z}$.

The total number of p-forms, for $p \geq 1$, is $\underset{\sim}{N}_p + \underset{\sim}{N}_{p-1}$, each associated with

- bottom p-cell: $w_i^p = (1 - \underset{\sim}{z})\, \Pi^* \underset{\sim}{w}_i^p$ for $i = 1, \ldots, \underset{\sim}{N}_p$;
- side p-cell: $w_{\underset{\sim}{N}_p + i}^p = \underset{\sim}{z} \mathrm{d} w_i^{p-1} - p\, \mathrm{d}\underset{\sim}{z} \wedge w_i^{p-1}$ for $i = 1, \ldots, \underset{\sim}{N}_{p-1}$.

Bossavit [7] has proved that w_i^p satisfies the definition of Whitney forms (1) on K and the following property:

Lemma 3.3 *If $M^p(\underset{\sim}{K}) = span\{\underset{\sim}{w}_i^p\}$ satisfies the discrete de Rham complex, then so does $M^p(K) = span\{w_i^p\}$ where w_i^ps are defined by either the conation or the extrusion.*

Finally, we mention the restriction of the projection $\pi : K \to \underset{\sim}{K}$ on a q-cell $\sigma \in K_q$ for $0 \le q \le m+1$. Denote $\underset{\sim}{\sigma} = \pi(\sigma) \subset \underset{\sim}{K}$. Then $\pi_\sigma \triangleq \pi|_\sigma$ maps σ to $\underset{\sim}{\sigma}$. One can similarly define the pushforward $(\pi_\sigma)_* : T_x\sigma \to T_{\underset{\sim}{x}}\underset{\sim}{\sigma}$ and the pullback $\pi_\sigma^* : \Lambda^p(\underset{\sim}{\sigma}) \to \Lambda^p(\sigma)$. We are interested in the situation when $\sigma \cap \underset{\sim}{K} = \underset{\sim}{\sigma}$, which can be further divided into two cases, as discussed in the following two remarks:

Remark 3.4 When $\sigma \subset \underset{\sim}{K}$, one has $\pi_\sigma = id$ and $\underset{\sim}{\sigma} = \sigma$. Consequently, both $(\pi_\sigma)_*$ and π_σ^* are identity operators.

Remark 3.5 When σ is a side q-cell and $\sigma \cap \underset{\sim}{K} = \underset{\sim}{\sigma}$ is a $(q-1)$-cell, one can similarly define a set of Whitney forms on σ using the extrusion/conation from the forms on $\underset{\sim}{\sigma}$, with π^* replaced by $(\pi_\sigma)^*$.

4 H^1, H(curl) and H(div) conforming finite elements on 3D prism/cone K

In this section, we show that the vector proxies of the Whitney forms w_i^p under the Cartesian coordinates, with $\underset{\sim}{K}$ being a 2D convex polygon and K being a 3D prism/cone, form a set of basis functions of H^1, $H(\text{curl})$ and $H(\text{div})$ conforming finite elements.

To this end, we first introduce the so-called vector proxy [2,22] of differential forms under the Cartesian coordinates. For example, the 2D Cartesian coordinate $\underset{\sim}{x}\,\underset{\sim}{y}$ provides a set of basis for p-forms on $\underset{\sim}{K}$, i.e., $\{\mathrm{d}\underset{\sim}{x}, \mathrm{d}\underset{\sim}{y}\}$ for 1-forms and $\{\mathrm{d}\underset{\sim}{x} \wedge \mathrm{d}\underset{\sim}{y}\}$ for 2-forms. Each p-form can be expressed as a linear combination of the basis, and its coefficients in the linear combination is called the vector proxy of the p-form under the Cartesian coordinate $\underset{\sim}{x}\,\underset{\sim}{y}$. The vector proxy of a 0-form is just the 0-form (scalar function) itself. In 3D, one can similarly define the vector proxy for p-forms, $p = 0, 1, 2, 3$. Formulae of the vector proxy for differential p-forms are listed in Table 1, together with the relation between the exterior derivative of a differential form and the gradient, rot/curl, divergence of its vector proxy. Note that in the table, we conveniently denote the vector proxy of a given differential form by replacing the lower case letter in its name into the upper case, while changing the font into a roman style. When the vector proxy is a vector-valued function, its name is printed in bold face. If the notation of the differential form carries any superscript, subscript, or accent, then so does the notation for its vector proxy. For example, the vector proxy for a differential 0-form $\underset{\sim}{w}$ is a scalar function $\underset{\sim}{\mathrm{W}}$, and the vector proxy for a Whitney 1-form w_i^1 is a vector-valued function $\mathbf{W}_i^1$.

Using the above notation, we get the vector proxy for the Whitney forms w_i^p listed in Sect. 3. By the definition (1), one clearly has:

Table 1 Vector proxy of differential p-forms in 2D and 3D

2D			
p	$\underset{\sim}{w} \in \Lambda^p(\underset{\sim}{K})$	vector proxy for $\underset{\sim}{w}$	for $\mathrm{d}\underset{\sim}{w}$
0	$\underset{\sim}{f}$	$\underset{\sim}{\mathrm{W}} = \underset{\sim}{f}$	$\nabla\underset{\sim}{\mathrm{W}}$
1	$\underset{\sim}{f}\mathrm{d}\underset{\sim}{x} + \underset{\sim}{g}\mathrm{d}\underset{\sim}{y}$	$\underset{\sim}{\mathbf{W}} = (\underset{\sim}{f}, \underset{\sim}{g})^t$	$\mathrm{rot}\,\underset{\sim}{\mathbf{W}}$
2	$\underset{\sim}{f}\mathrm{d}\underset{\sim}{x} \wedge \mathrm{d}\underset{\sim}{y}$	$\underset{\sim}{\mathrm{W}} = \underset{\sim}{f}$	0
3D			
p	$w \in \Lambda^p(K)$	vector proxy for w	for $\mathrm{d}w$
0	f	$\mathrm{W} = f$	$\nabla\mathrm{W}$
1	$f\mathrm{d}x + g\mathrm{d}y + h\mathrm{d}z$	$\mathbf{W} = (f, g, h)^t$	$\nabla \times \mathbf{W}$
2	$f\mathrm{d}y \wedge \mathrm{d}z + g\mathrm{d}z \wedge \mathrm{d}x + h\mathrm{d}x \wedge \mathrm{d}y$	$\mathbf{W} = (f, g, h)^t$	$\nabla \cdot \mathbf{W}$
3	$f\mathrm{d}x \wedge \mathrm{d}y \wedge \mathrm{d}z$	$\mathrm{W} = f$	0

Table 2 Vector proxy of wedge products in 3D

Differential forms w and u	Vector proxy of $w \wedge u$
$w, u \in \Lambda^1(K)$	$\mathbf{W} \times \mathbf{U}$
$w \in \Lambda^1(K), u \in \Lambda^2(K)$	$\mathbf{W} \cdot \mathbf{U}$

Note that 0-form wedge any other differential form can be treated as multiplication, and the wedge product of two 2-forms is 0

Lemma 4.1 *The vector proxies $\mathbf{W}_i^p$, for $p = 0, \ldots, 3$ and $i = 1, \ldots, N^p$ satisfy*

$$\begin{aligned}
\mathrm{W}_i^0(\boldsymbol{v}_j) &= \delta_{ij}, && \text{for all vertices } \boldsymbol{v}_j \in K_0,\\
\int_{e_j} \mathbf{W}_i^1 \cdot \boldsymbol{t}_j \,\mathrm{d}s &= \delta_{ij}, && \text{for all edges } e_j \in K_1,\\
\int_{F_j} \mathbf{W}_i^2 \cdot \boldsymbol{n}_j \,\mathrm{d}A &= \delta_{ij}, && \text{for all faces } F_j \in K_2,\\
\int_K \mathrm{W}_i^3 \,\mathrm{d}V &= 1,
\end{aligned}$$

with $\boldsymbol{t}_i$ and $\boldsymbol{n}_j$ being the unit tangential and unit normal vectors on e_i and F_j, respectively.

In Table 2, we list how to calculate wedge products of differential forms by using vector proxies.

Recall that π is not well-defined at the apex when K is a cone, as discussed in Remark 3.1. In order to use the vector proxy of w_i^p as finite element basis, we state the following lemma:

Lemma 4.2 *The vector proxies of w_i^p, for $p = 0, \ldots, 3$ and $i = 1, \ldots, N^p$, can be extended continuously to the boundary of K.*

Proof The lemma can be proved by calculation. Therefore it will become clear after Sect. 5, in which we give formulae for the vector proxies. □

Lemmas 4.1-4.2 do not automatically guarantee that the finite element spaces built upon these basis functions are conforming. This is different from the case when K is a simplex, in which the Whitney forms consist of polynomials and thus conformity can be easily achieved by examining the unisolvency of polynomials. On polygon-based prisms/cones, the basis functions may no longer be polynomials and thus the conformity of the finite element space must be carefully examined.

The H^1, $H(\mathrm{curl})$ and $H(\mathrm{div})$ conformity requires, respectively, that the function value, the tangential component, and the normal component to be continuous across the interface between mesh elements. Therefore we need to first define the "trace" (restriction) of differential forms on the boundary of K. Let $\sigma \in K_q$ be a q-cell. There is a natural inclusion $id_\sigma : \sigma \to K$. The natural inclusion thus induces a pullback $id_\sigma^* : \Lambda^p(K) \to \Lambda^p(\sigma)$ for all $p \geq 0$. Note that $id_\sigma^* = 0$ for $p > q$ since in this case $\Lambda^p(\sigma) = \{0\}$. We name this pullback the "trace" of forms on σ, and denote $\mathrm{Tr}_\sigma = id_\sigma^*$. One can similarly define the trace $\mathrm{Tr}_{\tilde{\sigma}} : \Lambda^p(\underset{\sim}{K}) \to \Lambda^p(\tilde{\sigma})$ as the pullback of the natural inclusion $id_{\tilde{\sigma}} : \tilde{\sigma} \to \underset{\sim}{K}$. Then, we have the following commutative property:

Lemma 4.3 *Let σ be a sub-cell of K satisfying $\sigma \cap \underset{\sim}{K} = \tilde{\sigma}$. One has*

$$\mathrm{Tr}_\sigma \circ \pi^* = \pi_\sigma^* \circ \mathrm{Tr}_{\tilde{\sigma}}.$$

Proof The lemma follows immediately from the definitions of pushforward, pullback, and the fact that $\pi \circ id_\sigma(\boldsymbol{x}) = id_{\tilde{\sigma}} \circ \pi_\sigma(\boldsymbol{x})$ for all $\boldsymbol{x} \in \sigma$. □

Corollary 4.4 *When $\sigma \subset \underset{\sim}{K}$, one has $\mathrm{Tr}_\sigma \circ \pi^* = \mathrm{Tr}_{\tilde{\sigma}}$. In particular, when $\sigma = \underset{\sim}{K}$, one has $\mathrm{Tr}_\sigma \circ \pi^* = id$.*

Proof Note that when $\sigma \subset \underset{\sim}{K}$, the operator π_σ^* becomes identity; and when $\sigma = \underset{\sim}{K}$, the operator $\mathrm{Tr}_{\tilde{\sigma}}$ also becomes identity. Then the result follows directly from Lemma 4.3. □

Remark 4.5 The trace operator satisfies all properties of pullbacks. For example, it is compatible with both the exterior product and the exterior derivative, i.e., similar to (5).

Remark 4.6 For $\eta^0 \in \Lambda^0(K)$, one has $\mathrm{Tr}_\sigma \eta^0 = \eta^0|_\sigma$. For $\underset{\sim}{\eta}{}^0 \in \Lambda^0(\underset{\sim}{K})$, one has $\mathrm{Tr}_{\tilde{\sigma}} \underset{\sim}{\eta}{}^0 = \underset{\sim}{\eta}{}^0|_{\tilde{\sigma}}$. For simplicity, we often write $\mathrm{Tr}_\sigma \eta^0 = \eta^0$ and $\mathrm{Tr}_{\tilde{\sigma}} \underset{\sim}{\eta}{}^0 = \underset{\sim}{\eta}{}^0$, when there is no ambiguity.

It is not hard to derive the relation between the trace of a differential form and its vector proxy, which we list in Table 3. The table immediately shows that the H^1, $H(\mathrm{curl})$ and $H(\mathrm{div})$ conformity of the vector proxy can be achieved as long as the

Table 3 Trace of a differential form $w \in \Lambda^p(K)$ on a sub-cell σ

$Tr_\sigma w$	$w \in \Lambda^0(K)$	$w \in \Lambda^1(K)$	$w \in \Lambda^2(K)$	$w \in \Lambda^3(K)$
$\sigma \in K_0$	$w\|_\sigma$	0	0	0
$\sigma \in K_1$	$w\|_\sigma$	$\mathbf{W}\|_\sigma \cdot \boldsymbol{t}\,\mathrm{d}t$	0	0
$\sigma \in K_2$	$w\|_\sigma$	$\mathbf{W}\|_\sigma \cdot \boldsymbol{t}_1\,\mathrm{d}t_1$ $+\mathbf{W}\|_\sigma \cdot \boldsymbol{t}_2\,\mathrm{d}t_2$	$\mathbf{W}\|_\sigma \cdot \boldsymbol{n}\,\mathrm{d}t_1 \wedge \mathrm{d}t_2$	0
$\sigma \in K_3$	w	w	w	w

Here we denote by W or $\mathbf{W}$ the vector proxy of the differential form $w \in \Lambda^p(K)$. When $\sigma \in K_1$, we parametrize σ by $0 \le t \le 1$ and denote by $\boldsymbol{t}$ the unit tangential vector. When $\sigma \in K_2$, we denote by t_1t_2 a Cartesian coordinate system on σ that is compatible with the orientation of σ, and $\boldsymbol{n}$ the normal direction

traces of the Whitney forms are continuous across adjacent mesh elements. To this end, we first examine the effect of $\mathrm{Tr}_{\tilde{\sigma}}$ on the Whitney forms $\tilde{w}_i^p$ defined on $\tilde{K}$, for $p = 0, 1, 2$.

Lemma 4.7 *Let $\tilde{\sigma} \in \tilde{K}_q$ for $q = 0, 1, 2$. Then one has $\mathrm{Tr}_{\tilde{\sigma}} \tilde{w}_i^p \in M^p(\tilde{\sigma})$, for $p = 0, 1, 2$.*

Proof When $q = 2$, one has $\tilde{\sigma} = \tilde{K}$ and Corollary 4.4 implies that $\mathrm{Tr}_{\tilde{\sigma}} \tilde{w}_i^p = \tilde{w}_i^p \in M^p(\tilde{K})$. When $q = 0$, we know that $\mathrm{Tr}_{\tilde{\sigma}} \tilde{w}_i^0 = \tilde{w}_i^0|_{\tilde{\sigma}} \in \mathbb{R} = M^0(\tilde{\sigma})$ and $\mathrm{Tr}_{\tilde{\sigma}} \tilde{w}_i^p = 0 \in M^p(\tilde{\sigma})$, for $p = 1, 2$. Now let us check the case when $q = 1$, i.e., $\tilde{\sigma}$ is an edge of $\tilde{K}$. Let $\tilde{\sigma}$ be parametrized by $0 \le t \le 1$, and denote by $\boldsymbol{t}$, $\boldsymbol{n}$ the unit tangential and unit normal vectors on $\tilde{\sigma}$ so that $\boldsymbol{n}$ and $\boldsymbol{t}$ form a positively oriented coordinate system. Clearly $\mathrm{Tr}_{\tilde{\sigma}} \tilde{w}_i^0 = \tilde{w}_i^0|_{\tilde{\sigma}}$ is a linear function on $\tilde{\sigma}$ and hence lies in $M^0(\tilde{\sigma})$, and $\mathrm{Tr}_{\tilde{\sigma}} \tilde{w}_i^2 = 0 \in M^2(\tilde{\sigma})$. So we only need to check $\mathrm{Tr}_{\tilde{\sigma}} \tilde{w}_i^1$. Note that by simple calculation one gets

$$\begin{bmatrix} \mathrm{Tr}_{\tilde{\sigma}} \mathrm{d}\tilde{x} \\ \mathrm{Tr}_{\tilde{\sigma}} \mathrm{d}\tilde{y} \end{bmatrix} = |\tilde{\sigma}|\boldsymbol{t}\mathrm{d}t,$$

where $|\tilde{\sigma}|$ is the length of $\tilde{\sigma}$. By Equation (3) and Lemma 2.2, we have

$$\begin{aligned}
\mathrm{Tr}_{\tilde{\sigma}} \tilde{w}_i^1 &= \mathrm{Tr}_{\tilde{\sigma}} \left(\frac{-[\boldsymbol{q}_i]_2}{|\tilde{e}_i|} \mathrm{d}\tilde{x} + \frac{[\boldsymbol{q}_i]_1}{|\tilde{e}_i|} \mathrm{d}\tilde{y} \right) \\
&= \frac{-[\boldsymbol{q}_i]_2}{|\tilde{e}_i|}\bigg|_{\tilde{\sigma}} \mathrm{Tr}_{\tilde{\sigma}} \mathrm{d}\tilde{x} + \frac{[\boldsymbol{q}_i]_1}{|\tilde{e}_i|}\bigg|_{\tilde{\sigma}} \mathrm{Tr}_{\tilde{\sigma}} \mathrm{d}\tilde{y} = \begin{bmatrix} \frac{-[\boldsymbol{q}_i]_2}{|\tilde{e}_i|} & \frac{[\boldsymbol{q}_i]_1}{|\tilde{e}_i|} \end{bmatrix}\bigg|_{\tilde{\sigma}} \begin{bmatrix} \mathrm{Tr}_{\tilde{\sigma}} \mathrm{d}\tilde{x} \\ \mathrm{Tr}_{\tilde{\sigma}} \mathrm{d}\tilde{y} \end{bmatrix} \\
&= \left(\frac{|\tilde{\sigma}|}{|\tilde{e}_i|} \boldsymbol{q}_i \cdot \boldsymbol{n} \mathrm{d}t \right)\bigg|_{\tilde{\sigma}} = \begin{cases} \mathrm{d}t & \text{if } \tilde{\sigma} = \tilde{e}_i \text{ with the same orientation} \\ -\mathrm{d}t & \text{if } \tilde{\sigma} = \tilde{e}_i \text{ but with different orientation} \\ 0 & \text{otherwise} \end{cases} \\
&\in M^1(\tilde{\sigma}),
\end{aligned}$$

where $\tilde{e}_i$ is the ith edge of $\tilde{K}$. This completes the proof of the lemma. □

Now we are able to prove the main theorem of this section.

Theorem 4.8 *Given that the generalized barycentric coordinates satisfy (4), on each q-cell $\sigma \in K_q$, for $0 \le q \le 3$, one has*

$$\mathrm{Tr}_\sigma\, w_i^p \in M^p(\sigma) \quad \text{for } p = 0, 1, 2, 3 \text{ and } i = 1, \ldots, N_p. \tag{6}$$

Proof From Table 3, it is clear that (6) is automatically true for $q = 3$ or $p > q$. For $q = 0$, i.e., σ is a vertex, one has $\mathrm{Tr}_\sigma\, w_i^0 = w_i^0|_\sigma \in \mathbb{R} = M^0(\sigma)$ and hence (6) is also true. Therefore, we only need to prove (6) for σ being 1- and 2-cells, and $p \le q$.

Case 1: conation.

1. When σ is a bottom edge, by Corollary 4.4 and remarks 4.5-4.6, one has for $i = 1, \ldots, n$,

$$\begin{aligned}
\mathrm{Tr}_\sigma\, w_i^0 &= \mathrm{Tr}_\sigma\left((1-\underset{\sim}{z})\,\pi^* \underset{\sim}{w}_i^0\right) = (1-0)\,\mathrm{Tr}_{\underset{\sim}{\sigma}}\, \underset{\sim}{w}_i^0 = \mathrm{Tr}_{\underset{\sim}{\sigma}}\, \underset{\sim}{w}_i^0,\\
\mathrm{Tr}_\sigma\, w_{n+1}^0 &= \mathrm{Tr}_\sigma\, \underset{\sim}{z} = 0,\\
\mathrm{Tr}_\sigma\, w_i^1 &= \mathrm{Tr}_\sigma\left((1-\underset{\sim}{z})^2\,\pi^* \underset{\sim}{w}_i^1\right) = (1-0)^2\,\mathrm{Tr}_{\underset{\sim}{\sigma}}\, \underset{\sim}{w}_i^1 = \mathrm{Tr}_{\underset{\sim}{\sigma}}\, \underset{\sim}{w}_i^1,\\
\mathrm{Tr}_\sigma\, w_{n+i}^1 &= \underset{\sim}{z}|_\sigma \mathrm{Tr}_\sigma(\mathrm{d}w_i^0) - \mathrm{Tr}_\sigma(\mathrm{d}\underset{\sim}{z}) \wedge \mathrm{Tr}_\sigma\, w_i^0 = 0 - \mathrm{d}(\mathrm{Tr}_\sigma\, \underset{\sim}{z}) \wedge \mathrm{Tr}_\sigma\, w_i^0\\
&= -\mathrm{d}(0) \wedge \mathrm{Tr}_\sigma\, w_i^0 = 0.
\end{aligned}$$

   Then, according to Lemma 4.7 and noticing that $\underset{\sim}{\sigma} = \sigma$, Equation (6) holds for Whitney 0- and 1-forms.

2. Consider the case when σ is a side edge. Then $\underset{\sim}{\sigma}$ is a vertex. For a constant-valued 0-form $c \in \mathbb{R}$ defined on $\underset{\sim}{\sigma}$, it is not hard to see that $\pi_\sigma^*(c) = c$, where the right-hand side is viewed as a constant-valued function on σ. By Lemma 4.3 and remarks 4.5-4.6, one has for $i = 1, \ldots, n$,

$$\begin{aligned}
\mathrm{Tr}_\sigma\, w_i^0 &= \mathrm{Tr}_\sigma\left((1-\underset{\sim}{z})\,\pi^* \underset{\sim}{w}_i^0\right) = (1-\underset{\sim}{z})|_\sigma\, (\pi_\sigma^* \mathrm{Tr}_{\underset{\sim}{\sigma}}\, \underset{\sim}{w}_i^0)\\
&= (1-\underset{\sim}{z})|_\sigma\, \pi_\sigma^*\left(\underset{\sim}{w}_i^0|_{\underset{\sim}{\sigma}}\right) = (1-\underset{\sim}{z})|_\sigma\, \underset{\sim}{w}_i^0|_{\underset{\sim}{\sigma}}\\
&= \begin{cases} (1-\underset{\sim}{z})|_\sigma & \text{if } \sigma \text{ is the ith side edge}\\ 0 & \text{otherwise} \end{cases},\\
\mathrm{Tr}_\sigma\, w_{n+1}^0 &= \mathrm{Tr}_\sigma\, \underset{\sim}{z} = \underset{\sim}{z}|_\sigma,\\
\mathrm{Tr}_\sigma\, w_i^1 &= \mathrm{Tr}_\sigma\left((1-\underset{\sim}{z})^2\,\pi^* \underset{\sim}{w}_i^1\right) = (1-\underset{\sim}{z})^2|_\sigma\, (\pi_\sigma^* \mathrm{Tr}_{\underset{\sim}{\sigma}}\, \underset{\sim}{w}_i^1) = 0,\\
&\qquad\qquad \text{(Since } \underset{\sim}{\sigma} \text{ is a 0-cell, one has } \mathrm{Tr}_{\underset{\sim}{\sigma}}\, \underset{\sim}{w}_i^1 = 0.)\\
\mathrm{Tr}_\sigma\, w_{n+i}^1 &= \underset{\sim}{z}|_\sigma \mathrm{d}(\mathrm{Tr}_\sigma\, w_i^0) - \mathrm{d}(\underset{\sim}{z}|_\sigma) \wedge \mathrm{Tr}_\sigma\, w_i^0\\
&= \begin{cases} \underset{\sim}{z}|_\sigma \mathrm{d}(1-\underset{\sim}{z})|_\sigma - \mathrm{d}(\underset{\sim}{z}|_\sigma)(1-\underset{\sim}{z})|_\sigma = -\mathrm{d}\underset{\sim}{z}|_\sigma & \\ \qquad\qquad\qquad\qquad \text{if } \sigma \text{ is the ith side edge} & \\ 0 \qquad\qquad\qquad\qquad \text{otherwise} & \end{cases}.
\end{aligned}$$

   Following the discussion of $M^p(\sigma)$ at the end of Sect. 2, clearly $(1-\underset{\sim}{z})|_\sigma$ and $\underset{\sim}{z}|_\sigma$ are linear scalar functions on σ and hence both lie in $M^0(\sigma)$. Similarly, $-\mathrm{d}\underset{\sim}{z}|_\sigma$ is

a constant-valued 1-form on σ and hence lies in $M^1(\sigma)$. Thus Equation (6) holds for Whitney 0- and 1-forms.

3. When $\sigma = \underset{\sim}{K}$ is the bottom face, by Corollary 4.4 and remarks 4.5-4.6, one has for $i = 1, \ldots, n$,

$$\begin{aligned}
\mathrm{Tr}_\sigma w_i^0 &= (1 - \underset{\sim}{z})|_\sigma \, (\mathrm{Tr}_\sigma \pi^* \underset{\sim}{w}_i^0) = \underset{\sim}{w}_i^0 \in M^0(\sigma), \\
\mathrm{Tr}_\sigma w_{n+1}^0 &= \underset{\sim}{z}|_\sigma = 0, \\
\mathrm{Tr}_\sigma w_i^1 &= (1 - \underset{\sim}{z})^2|_\sigma \, (\mathrm{Tr}_\sigma \pi^* \underset{\sim}{w}_i^1) = \underset{\sim}{w}_i^1 \in M^1(\sigma), \\
\mathrm{Tr}_\sigma w_{n+i}^1 &= \underset{\sim}{z}|_\sigma \, \mathrm{d}(w_i^0|_\sigma) - \mathrm{d}(\underset{\sim}{z}|_\sigma) \wedge (w_i^0|_\sigma) = 0 - 0 \wedge w_i^0|_\sigma = 0, \\
\mathrm{Tr}_\sigma w_1^2 &= (1 - \underset{\sim}{z})^3|_\sigma \, (\mathrm{Tr}_\sigma \pi^* \underset{\sim}{w}_1^2) = \underset{\sim}{w}_1^2 \in M^2(\sigma), \\
\mathrm{Tr}_\sigma w_{1+i}^2 &= \underset{\sim}{z}|_\sigma \, \mathrm{d}(\mathrm{Tr}_\sigma w_i^1) - 2\mathrm{d}(\underset{\sim}{z}|_\sigma) \wedge \mathrm{Tr}_\sigma w_i^1 = 0 - 0 \wedge \mathrm{Tr}_\sigma w_i^1 = 0.
\end{aligned}$$

4. The most complicated case is when σ is a side face. For simplicity, we parametrize the edge $\underset{\sim}{\varsigma}$ by variable t, and denote by $\lambda_i, i = 1, 2, 3$, the barycentric coordinates on the triangle σ with the third vertex being the apex. Then one clearly has $\lambda_3 = \underset{\sim}{z}|_\sigma$. For $i = 1, \ldots, n$, one gets

$$\mathrm{Tr}_\sigma w_i^0 = (1 - \underset{\sim}{z})|_\sigma \, \pi_\sigma^* (\mathrm{Tr}_{\underset{\sim}{\varsigma}} \underset{\sim}{w}_i^0),$$

which by Remark 3.5 is just the conation formula from $\underset{\sim}{\varsigma}$ to σ. The conation from a line segment to a triangle gives exactly the traditional Whitney forms on the triangle [7]. Thus $\mathrm{Tr}_\sigma w_i^0 \in M^0(\sigma)$. Next, for w_{n+1}^0, we have

$$\mathrm{Tr}_\sigma w_{n+1}^0 = \underset{\sim}{z}|_\sigma \in M^0(\sigma),$$

because the Whitney 0-forms on a triangle are known to span all linear functions.

Similarly, for $i = 1, \ldots, n$, we have

$$\begin{aligned}
\mathrm{Tr}_\sigma w_i^1 &= (1 - \underset{\sim}{z})^2|_\sigma \, \pi_\sigma^* (\mathrm{Tr}_{\underset{\sim}{\varsigma}} \underset{\sim}{w}_i^1) \\
&= \begin{cases} (1 - \underset{\sim}{z})^2|_\sigma \pi_\sigma^* \mathrm{Tr}_{\underset{\sim}{\varsigma}} (c\mathrm{d}t) & \text{if } \sigma \text{ is the ith side face} \\ 0 & \text{otherwise} \end{cases}.
\end{aligned}$$

Again by Remark 3.5, the right-hand side is just the conation formula from the edge $\underset{\sim}{\varsigma}$ to the triangle σ. Hence $\mathrm{Tr}_\sigma w_i^1 \in M^1(\sigma)$. For w_{n+i}^1, we have

$$\begin{aligned}
\mathrm{Tr}_\sigma w_{n+i}^1 &= \underset{\sim}{z}|_\sigma \mathrm{d}(\mathrm{Tr}_\sigma w_i^0) - \mathrm{d}(\mathrm{Tr}_\sigma \underset{\sim}{z}) \wedge \mathrm{Tr}_\sigma w_i^0 \\
&= \begin{cases} 0 & \text{if the ith vertex is not in } \sigma \\ \lambda_3 \mathrm{d}\lambda_1 - \lambda_1 \mathrm{d}\lambda_3 & \text{if the ith vertex is the first vertex of } \sigma \\ \lambda_3 \mathrm{d}\lambda_2 - \lambda_2 \mathrm{d}\lambda_3 & \text{if the ith vertex is the second vertex of } \sigma \end{cases}.
\end{aligned}$$

It is well known that the forms $\lambda_k \mathrm{d}\lambda_j - \lambda_j \mathrm{d}\lambda_k$, for $1 \le j, k \le 3$, define Whitney 1-forms on a triangle. Thus one has $\mathrm{Tr}_\sigma w^1_{n+i} \in M^1(\sigma)$.
Finally,

$$\begin{aligned} \mathrm{Tr}_\sigma w^2_1 &= (1 - \underset{\sim}{z})^3|_\sigma \pi^*_\sigma(\mathrm{Tr}_{\underset{\sim}{\sigma}} \underset{\sim}{w}^2_1) = (1 - \underset{\sim}{z})^3|_\sigma \pi^*_\sigma(0) = 0, \\ \mathrm{Tr}_\sigma w^2_{1+i} &= \underset{\sim}{z}|_\sigma \, \mathrm{d}(\mathrm{Tr}_\sigma w^1_i) - 2\mathrm{d}(\underset{\sim}{z}|_\sigma) \wedge \mathrm{Tr}_\sigma w^1_i. \end{aligned}$$

We have previously proved that $\mathrm{Tr}_\sigma w^1_i \in M^1(\sigma)$. Note that the above expression for $\mathrm{Tr}_\sigma w^2_{1+i}$ is again the conation formula from the line segment $\underset{\sim}{\sigma}$ to the triangle σ. Thus by [7] one has $\mathrm{Tr}_\sigma w^2_{1+i} \in M^2(\sigma)$.

Case 2: extrusion
Computation for the extrusion case is similar but much easier than the conation case. One just needs to be careful that when σ is a side face, the extrusion from $\underset{\sim}{\sigma}$ to σ generates the Whitney forms corresponding to the lowest-order Raviart–Thomas element on rectangles [7]. By Lemma 2.4, Eq. (4) is required in order to make sure that (6) holds. We skip the details of the proof. □

Combined with Table 3, Theorem 4.8 immediately implies that the vector proxies of the Whitney 0-, 1- and 2-forms on the prism/cone K form the basis of H^1, $H(\mathrm{curl})$ and $H(\mathrm{div})$ conforming finite elements, as the traces of the Whitney forms on a shared vertex/edge/face σ lie in $M^p(\sigma)$, which can be completely determined by the degrees of freedom associated with σ.

5 Efficient implementation

In [7], Bossavit discussed how to use extrusion and conation to compute Whitney forms on triangular- or rectangular-based prisms/cones via individual examples. Here we show how to efficiently and systematically implement the Whitney p-forms and their exterior derivatives on polygon-based prisms/cones.

Different from traditional finite element implementations, we do not explicitly calculate the analytical expression of the Whitney p-forms. Instead, implementation is done by following the extrusion/conation formula. In finite element methods, one uses Gaussian quadratures to approximate integrals on a mesh component, which involves the evaluation of finite element basis functions (the shape functions) and their differentials at given Gaussian points. Note that on polygons/polyhedra, one can always subdivide the polygon/polyhedron into simplices and use simplicial Gaussian quadratures to do the numerical integration. Now the implementation reduces to evaluating the shape functions and their corresponding exterior derivatives at individual Gaussian points. The evaluation can thus be done by following the extrusion/conation formulae. In this process, two main issues need to be addressed: the calculation of the pull-back π^* and the calculation of the exterior derivatives.

5.1 Computing the pullback operator

Pullback of 0-forms is easy to calculate since 0-forms are just scalar functions. Let $\underset{\sim}{f}$ be a 0-form (scalar function) on $\underset{\sim}{K}$. Usually $\underset{\sim}{f}$ is given as a function of $\underset{\sim}{\boldsymbol{x}}$. Therefore one has

$$(\pi^* \underset{\sim}{f})(\boldsymbol{x}) = \underset{\sim}{f} \circ \pi(\boldsymbol{x}) = \underset{\sim}{f}(\underset{\sim}{\boldsymbol{x}}),$$

which is exactly the same expression as $\underset{\sim}{f}$ in terms of $\underset{\sim}{\boldsymbol{x}}$, for both the extrusion and the conation. For simplicity, we write informally

$$\pi^* \underset{\sim}{f} = \underset{\sim}{f},$$

in the rest of this section, while keeping in mind that $\underset{\sim}{f}$ is a function of $\underset{\sim}{\boldsymbol{x}} = \pi(\boldsymbol{x})$. For any p-form $\underset{\sim}{w}$ on $\underset{\sim}{K}$, one has

$$\pi^*(\underset{\sim}{f}\,\underset{\sim}{w}) = (\pi^* \underset{\sim}{f})(\pi^* \underset{\sim}{w}) = (\underset{\sim}{f})(\pi^* \underset{\sim}{w}).$$

For 1-forms and 2-forms, by basic chain rules one gets

$$\begin{bmatrix} \pi^* \mathrm{d}\underset{\sim}{x} \\ \pi^* \mathrm{d}\underset{\sim}{y} \end{bmatrix} = \frac{\partial(\underset{\sim}{x}, \underset{\sim}{y})}{\partial(x, y, z)} \begin{bmatrix} \mathrm{d}x \\ \mathrm{d}y \\ \mathrm{d}z \end{bmatrix} = \begin{bmatrix} \frac{\partial \underset{\sim}{x}}{\partial x} & \frac{\partial \underset{\sim}{x}}{\partial y} & \frac{\partial \underset{\sim}{x}}{\partial z} \\ \frac{\partial \underset{\sim}{y}}{\partial x} & \frac{\partial \underset{\sim}{y}}{\partial y} & \frac{\partial \underset{\sim}{y}}{\partial z} \end{bmatrix} \begin{bmatrix} \mathrm{d}x \\ \mathrm{d}y \\ \mathrm{d}z \end{bmatrix},$$

$$\pi^*(\mathrm{d}\underset{\sim}{x} \wedge \mathrm{d}\underset{\sim}{y}) = \left| \frac{\partial(\underset{\sim}{x}, \underset{\sim}{y})}{\partial(x, y)} \right| \mathrm{d}x \wedge \mathrm{d}y + \left| \frac{\partial(\underset{\sim}{x}, \underset{\sim}{y})}{\partial(x, z)} \right| \mathrm{d}x \wedge \mathrm{d}z + \left| \frac{\partial(\underset{\sim}{x}, \underset{\sim}{y})}{\partial(y, z)} \right| \mathrm{d}y \wedge \mathrm{d}z,$$

where $|\cdot|$ denotes the determinant of Jacobian matrices. Then, the pullback of a 1-form $\underset{\sim}{f}\mathrm{d}\underset{\sim}{x} + \underset{\sim}{g}\mathrm{d}\underset{\sim}{y}$ is

$$\pi^*(\underset{\sim}{f}\mathrm{d}\underset{\sim}{x} + \underset{\sim}{g}\mathrm{d}\underset{\sim}{y}) = \begin{bmatrix} \pi^* \underset{\sim}{f} & \pi^* \underset{\sim}{g} \end{bmatrix} \begin{bmatrix} \pi^* \mathrm{d}\underset{\sim}{x} \\ \pi^* \mathrm{d}\underset{\sim}{y} \end{bmatrix} = \begin{bmatrix} \underset{\sim}{f} & \underset{\sim}{g} \end{bmatrix} \frac{\partial(\underset{\sim}{x}, \underset{\sim}{y})}{\partial(x, y, z)} \begin{bmatrix} \mathrm{d}x \\ \mathrm{d}y \\ \mathrm{d}z \end{bmatrix}.$$

Similarly, the pullback of a 2-form $\underset{\sim}{f}\,\mathrm{d}\underset{\sim}{x} \wedge \mathrm{d}\underset{\sim}{y}$ is

$$\begin{aligned} \pi^*(\underset{\sim}{f}\,\mathrm{d}\underset{\sim}{x} \wedge \mathrm{d}\underset{\sim}{y}) = \underset{\sim}{f} \Bigg(& \left| \frac{\partial(\underset{\sim}{x}, \underset{\sim}{y})}{\partial(x, y)} \right| \mathrm{d}x \wedge \mathrm{d}y \\ & + \left| \frac{\partial(\underset{\sim}{x}, \underset{\sim}{y})}{\partial(x, z)} \right| \mathrm{d}x \wedge \mathrm{d}z + \left| \frac{\partial(\underset{\sim}{x}, \underset{\sim}{y})}{\partial(y, z)} \right| \mathrm{d}y \wedge \mathrm{d}z \Bigg). \end{aligned}$$

Case 1: On prisms. From $\pi(\boldsymbol{x}) = \underset{\sim}{\boldsymbol{x}}$ and $\boldsymbol{x} = ext(\underset{\sim}{\boldsymbol{x}}, \underset{\sim}{z})$, one gets

$$\underset{\sim}{x} = x, \qquad \underset{\sim}{y} = y, \qquad \underset{\sim}{z} = \frac{1}{\theta} z. \tag{7}$$

Therefore the Jacobian matrices and determinants are

$$\frac{\partial(\underset{\sim}{x}, \underset{\sim}{y})}{\partial(x, y, z)} = \begin{bmatrix} 1 & 0 & 0 \\ 0 & 1 & 0 \end{bmatrix},$$
$$\left|\frac{\partial(\underset{\sim}{x}, \underset{\sim}{y})}{\partial(x, y)}\right| = 1, \qquad \left|\frac{\partial(\underset{\sim}{x}, \underset{\sim}{y})}{\partial(x, z)}\right| = \left|\frac{\partial(\underset{\sim}{x}, \underset{\sim}{y})}{\partial(y, z)}\right| = 0.$$

Consequently, one has

$$\begin{aligned} \pi^*(\underset{\sim}{f}\,\mathrm{d}\underset{\sim}{x} + \underset{\sim}{g}\mathrm{d}\underset{\sim}{y}) &= \underset{\sim}{f}\mathrm{d}x + \underset{\sim}{g}\mathrm{d}y, \\ \pi^*(\underset{\sim}{f}\mathrm{d}\underset{\sim}{x} \wedge \mathrm{d}\underset{\sim}{y}) &= \underset{\sim}{f}\mathrm{d}x \wedge \mathrm{d}y, \end{aligned} \tag{8}$$

for any 1-form $\underset{\sim}{f}\mathrm{d}\underset{\sim}{x} + \underset{\sim}{g}\mathrm{d}\underset{\sim}{y}$ and 2-form $\underset{\sim}{f}\mathrm{d}\underset{\sim}{x} \wedge \mathrm{d}\underset{\sim}{y}$.

Case 2: On cones. From $\tilde{\pi}(\boldsymbol{x}) = \underset{\sim}{\boldsymbol{x}}$ and $\tilde{\boldsymbol{x}} = con(\underset{\sim}{\boldsymbol{x}}, \underset{\sim}{z})$, one gets

$$\underset{\sim}{x} = \frac{x}{1 - \underset{\sim}{z}}, \qquad \underset{\sim}{y} = \frac{y}{1 - \underset{\sim}{z}}, \qquad \underset{\sim}{z} = \frac{1}{\theta}z. \tag{9}$$

Therefore the Jacobian matrices and determinants are

$$\frac{\partial(\underset{\sim}{x}, \underset{\sim}{y})}{\partial(x, y, z)} = \frac{1}{1 - \underset{\sim}{z}} \begin{bmatrix} 1 & 0 & \frac{1}{\theta}\underset{\sim}{x} \\ 0 & 1 & \frac{1}{\theta}\underset{\sim}{y} \end{bmatrix}, \qquad \left|\frac{\partial(\underset{\sim}{x}, \underset{\sim}{y})}{\partial(x, y)}\right| = \frac{1}{(1 - \underset{\sim}{z})^2},$$
$$\left|\frac{\partial(\underset{\sim}{x}, \underset{\sim}{y})}{\partial(x, z)}\right| = \frac{\underset{\sim}{y}}{\theta(1 - \underset{\sim}{z})^2}, \qquad \left|\frac{\partial(\underset{\sim}{x}, \underset{\sim}{y})}{\partial(y, z)}\right| = \frac{-\underset{\sim}{x}}{\theta(1 - \underset{\sim}{z})^2}.$$

Consequently, one has

$$\begin{aligned} \pi^*(\underset{\sim}{f}\mathrm{d}\underset{\sim}{x} + \underset{\sim}{g}\mathrm{d}\underset{\sim}{y}) &= \frac{1}{1 - \underset{\sim}{z}}\left(\underset{\sim}{f}\,\mathrm{d}x + \underset{\sim}{g}\,\mathrm{d}y + \frac{\underset{\sim}{x}\underset{\sim}{f} + \underset{\sim}{y}\underset{\sim}{g}}{\theta}\mathrm{d}z\right), \\ \pi^*(\underset{\sim}{f}\,\mathrm{d}\underset{\sim}{x} \wedge \mathrm{d}\underset{\sim}{y}) &= \frac{\underset{\sim}{f}}{(1 - \underset{\sim}{z})^2}\left(-\frac{\underset{\sim}{x}}{\theta}\mathrm{d}y \wedge \mathrm{d}z - \frac{\underset{\sim}{y}}{\theta}\mathrm{d}z \wedge \mathrm{d}x + \mathrm{d}x \wedge \mathrm{d}y\right), \end{aligned} \tag{10}$$

for any 1-form $\underset{\sim}{f}\mathrm{d}\underset{\sim}{x} + \underset{\sim}{g}\mathrm{d}\underset{\sim}{y}$ and 2-form $\underset{\sim}{f}\mathrm{d}\underset{\sim}{x} \wedge \mathrm{d}\underset{\sim}{y}$.

Although π^* is not well defined at $\underset{\sim}{z} = 1$, i.e., the apex, we point out that $(1 - \underset{\sim}{z})\Pi^* = (1-\underset{\sim}{z})^{p+1}\pi^*$ is well-defined on the entire K. Since the conation formulae use $(1-\underset{\sim}{z})\Pi^*$ in the definition, we conclude that the vector proxies of the Whitney forms, i.e., the finite element basis functions, can be extended continuously to the entire K.

5.2 Computing the exterior derivatives

The exterior derivatives of Whitney forms on prisms are easy to compute since their construction uses just tensor products. Therefore we only discuss here the computation on cones.

For 0-forms, we have for $1 \le i \le n$,

$$\begin{aligned} \mathrm{d}w_i^0 &= \mathrm{d}\left((1-\underset{\sim}{z})\pi^* \underset{\sim}{w}_i^0\right) = \mathrm{d}(1-\underset{\sim}{z}) \wedge \pi^* \underset{\sim}{w}_i^0 + (1-\underset{\sim}{z})\mathrm{d}(\pi^* \underset{\sim}{w}_i^0) \\ &= -(\pi^* \underset{\sim}{w}_i^0)\mathrm{d}\underset{\sim}{z} + (1-\underset{\sim}{z})\pi^*(\mathrm{d}\underset{\sim}{w}_i^0) \\ &= -(\Pi^* \underset{\sim}{w}_i^0)\mathrm{d}\underset{\sim}{z} + \Pi^*(\mathrm{d}\underset{\sim}{w}_i^0). \end{aligned}$$

And $\mathrm{d}w_{n+1}^0 = \mathrm{d}\underset{\sim}{z}$.

For 1-forms, we have for $1 \le i \le n$,

$$\begin{aligned} \mathrm{d}w_i^1 &= \mathrm{d}((1-\underset{\sim}{z})^2 \pi^* \underset{\sim}{w}_i^1) = \mathrm{d}(1-\underset{\sim}{z})^2 \wedge \pi^* \underset{\sim}{w}_i^1 + (1-\underset{\sim}{z})^2 \mathrm{d}(\pi^* \underset{\sim}{w}_i^1) \\ &= -\frac{2}{\theta}(1-\underset{\sim}{z})\mathrm{d}z \wedge \pi^* \underset{\sim}{w}_i^1 + (1-\underset{\sim}{z})^2 \pi^*(\mathrm{d}\underset{\sim}{w}_i^1) \\ &= -\frac{2}{\theta}\mathrm{d}z \wedge \Pi^* \underset{\sim}{w}_i^1 + \Pi^*(\mathrm{d}\underset{\sim}{w}_i^1), \end{aligned} \tag{11}$$

where in the second last step we used $\mathrm{d}\pi^* = \pi^* \mathrm{d}$. Using $\mathrm{d}^2 = 0$, one gets

$$\begin{aligned} \mathrm{d}w_{n+i}^1 &= \mathrm{d}(-\underset{\sim}{z}\mathrm{d}w_i^0 + w_i^0 \mathrm{d}\underset{\sim}{z}) \\ &= -\mathrm{d}\underset{\sim}{z} \wedge \mathrm{d}w_i^0 - \underset{\sim}{z}\mathrm{d}(\mathrm{d}w_i^0) + \mathrm{d}w_i^0 \wedge \mathrm{d}\underset{\sim}{z} + w_i^0 \wedge \mathrm{d}(\mathrm{d}\underset{\sim}{z}) \\ &= -2\mathrm{d}\underset{\sim}{z} \wedge \mathrm{d}w_i^0. \end{aligned}$$

For 2 forms, we have

$$\begin{aligned} \mathrm{d}w_1^2 &= \mathrm{d}((1-\underset{\sim}{z})^3 \pi^* \underset{\sim}{w}_1^2) = -\frac{3}{\theta}(1-\underset{\sim}{z})^2\, \mathrm{d}z \wedge \pi^* \underset{\sim}{w}_1^2 + (1-\underset{\sim}{z})^3 \pi^*(\mathrm{d}\underset{\sim}{w}_1^2) \\ &= -\frac{3}{\theta}(1-\underset{\sim}{z})^2\, \mathrm{d}z \wedge \pi^* \underset{\sim}{w}_1^2 \\ &= -\frac{3}{\theta}\mathrm{d}z \wedge \Pi^* \underset{\sim}{w}_1^2, \end{aligned}$$

and for $1 \le i \le n$

$$\begin{aligned} \mathrm{d}w_{1+i}^2 &= \mathrm{d}(\underset{\sim}{z}\mathrm{d}w_i^1 - 2\mathrm{d}\underset{\sim}{z} \wedge w_i^1) \\ &= \mathrm{d}\underset{\sim}{z} \wedge \mathrm{d}w_i^1 + 2\mathrm{d}\underset{\sim}{z} \wedge \mathrm{d}w_i^1. \end{aligned}$$

5.3 Efficient implementation using the vector proxy

With the formulae for the pullback operator, the exterior derivatives, and tables 1-2, one can easily evaluate the vector proxy of Whitney forms and their exterior derivatives at any given point $(x, y, z) \in K$, except for the apex when K is a cone. We shall illustrate the implementation with examples.

Remark 5.1 Although the basis functions are well defined at the apex when K is a cone, our implementation to be presented later does not work at the apex. This is because

the implementation requires the calculation of $(\underset{\sim}{x}, \underset{\sim}{y}, \underset{\sim}{z})$ from (x, y, z), which can not be done at the apex directly. This does not matter since usually one wants to evaluate the forms at Gaussian points while high-order Gaussian quadratures seldomly use the apex.

Example 1 compute $w_1^1 = (1 - \underset{\sim}{z})^2 \pi^* \underset{\sim}{w}_1^1$ at point (x, y, z) in a cone $K \backslash \{apex\}$.

1. Compute the unique scaled coordinate $(\underset{\sim}{x}, \underset{\sim}{y}, \underset{\sim}{z})$ satisfying $(x, y, z) = con(\underset{\sim}{x}, \underset{\sim}{y}, \underset{\sim}{z})$;
2. Evaluate $\underset{\sim}{w}_1^1$ at $(\underset{\sim}{x}, \underset{\sim}{y})$ using Lemma 2.2, and write its vector proxy as $[c_1, c_2]^t$ where $c_1, c_2 \in \mathbb{R}$;
3. Using the formula of the pullback (10), w_1^1 has the vector proxy

$$[(1 - \underset{\sim}{z})c_1,\ (1 - \underset{\sim}{z})c_2,\ (1 - \underset{\sim}{z})\frac{\underset{\sim}{x}c_1 + \underset{\sim}{y}c_2}{\theta}]^t.$$

Example 2 compute $\mathrm{d}w_1^1$ at point (x, y, z) in a cone $K \backslash \{apex\}$.

1. Compute the unique scaled coordinate $(\underset{\sim}{x}, \underset{\sim}{y}, \underset{\sim}{z})$ satisfying $(x, y, z) = con(\underset{\sim}{x}, \underset{\sim}{y}, \underset{\sim}{z})$;
2. Evaluate $\underset{\sim}{w}_1^1$ and $\mathrm{d}\underset{\sim}{w}_1^1$ at $(\underset{\sim}{x}, \underset{\sim}{y})$ using Lemma 2.2. Write the vector proxy for $\underset{\sim}{w}_1^1$ as $[c_1, c_2]^t$ where $c_1, c_2 \in \mathbb{R}$, and for $\mathrm{d}\underset{\sim}{w}_1^1$ as $c_d \in \mathbb{R}$;
3. Use (10) to evaluate the vector proxy for $\Pi^* \underset{\sim}{w}_1^1$, which is

$$[c_1,\ c_2,\ \frac{\underset{\sim}{x}c_1 + \underset{\sim}{y}c_2}{\theta}]^t,$$

and the vector proxy for $\Pi^*(\mathrm{d}\underset{\sim}{w}_1^1)$, which is

$$[\frac{-\underset{\sim}{x}c_d}{\theta},\ \frac{-\underset{\sim}{y}c_d}{\theta},\ c_d]^t;$$

4. Calculate the vector proxy of $\mathrm{d}z \wedge \Pi^* \underset{\sim}{w}_1^1$ as

$$\begin{bmatrix} 0 \\ 0 \\ 1 \end{bmatrix} \times \begin{bmatrix} c_1 \\ c_2 \\ \frac{\underset{\sim}{x}c_1 + \underset{\sim}{y}c_2}{\theta} \end{bmatrix} = \begin{bmatrix} -c_2 \\ c_1 \\ 0 \end{bmatrix};$$

5. Finally, use (11) to get the vector proxy of $\mathrm{d}w_1^1$, which is

$$-\frac{2}{\theta}\begin{bmatrix} -c_2 \\ c_1 \\ 0 \end{bmatrix} + \begin{bmatrix} \frac{-\underset{\sim}{x}c_d}{\theta} \\ \frac{-\underset{\sim}{y}c_d}{\theta} \\ c_d \end{bmatrix}.$$

6 Approximation property

In this section, we examine the approximation property of the space spanned by the p-forms. Since our finite element spaces are based on the generalized barycentric coordinates, it is natural to require that the mesh elements satisfy corresponding shape regularity assumptions for GBCs. Here we follow the shape regularity assumptions in [16,19], but skip the details as this is not the main concern of this paper. Then, according to the finite element theory, the key to the approximation error analysis is to prove that the vector-proxy of $M^p(K)$ contains the lowest-order Nédélec–Raviart–Thomas finite element spaces, respectively. More specifically, define on the prism/cone K the following spaces of p-forms, for $p = 0, 1, 2$,

$$\begin{aligned}
\mathcal{N}^0 &= span\{1,\ x,\ y,\ z\},\\
\mathcal{N}^1 &= \{f_1\mathrm{d}x + f_2\mathrm{d}y + f_3\mathrm{d}z,\ \text{for all } \boldsymbol{f} = \boldsymbol{a}\times\boldsymbol{x} + \boldsymbol{b} \text{ where } \boldsymbol{a}, \boldsymbol{b} \in \mathbb{R}^3\},\\
\mathcal{N}^2 &= \{f_1\mathrm{d}y\wedge\mathrm{d}z + f_2\mathrm{d}x\wedge\mathrm{d}x + f_3\mathrm{d}x\wedge\mathrm{d}y,\ \text{for all } \boldsymbol{f} = a\,\boldsymbol{x} + \boldsymbol{b}\\
&\qquad \text{where } a \in \mathbb{R},\ \boldsymbol{b} \in \mathbb{R}^3\}.
\end{aligned}$$

We shall show that $\mathcal{N}^p \subset M^p(K)$, for $p = 0, 1, 2$. Because the finite elements defined from $M^p(K)$ satisfies the discrete de Rham complex, as shown in Lemma 3.3, this guarantees that the elements have at least the same approximation rate as the lowest-order Nédélec–Raviart–Thomas elements.

First we prove the following lemma:

Lemma 6.1 *The set of Whitney* 0*-forms* $\{w_i^0\}$ *generated from extrusion/conation is a set of generalized barycentric coordinates on a prism/cone* K.

Proof It is not hard to see that all w_i^0s are non-negative functions. We only need to show that they satisfy the linear precision property (2).

First, consider the case when K is a prism. Note that $\sum_{i=1}^n \underset{\sim}{w}_i^0 = 1$, one immediately gets

$$\sum_{i=1}^n w_i^0 + \sum_{i=1}^n w_{n+i}^0 = \sum_{i=1}^n (1-\underset{\sim}{z})\pi^*\underset{\sim}{w}_i^0 + \sum_{i=1}^n \underset{\sim}{z}\pi^*\underset{\sim}{w}_i^0 = \pi^*(1) = 1.$$

Denote by $(x_i,\ y_i,\ 0)$, $1 \le i \le n$, the coordinates of bottom vertices, and by $(x_i,\ y_i,\ \theta)$, $1 \le i \le n$, the coordinates of top vertices. Since $\{\underset{\sim}{w}_i^0\}_{i=1}^n$ forms a set of generalized barycentric coordinates on the base polygon $\underset{\sim}{K}$ with vertices $(x_i,\ y_i)$,

we have

$$\begin{aligned}
&\sum_{i=1}^{n}\begin{bmatrix}x_i\\ y_i\\ 0\end{bmatrix} w_i^0+\sum_{i=1}^{n}\begin{bmatrix}x_i\\ y_i\\ \theta\end{bmatrix} w_{n+i}^0\\
&\quad=(1-\underset{\sim}{z})\pi^*\left(\sum_{i=1}^{n}\begin{bmatrix}x_i\\ y_i\\ 0\end{bmatrix}\underset{\sim}{w}_i^0\right)+\underset{\sim}{z}\pi^*\left(\sum_{i=1}^{n}\begin{bmatrix}x_i\\ y_i\\ \theta\end{bmatrix}\underset{\sim}{w}_i^0\right)\\
&\quad=(1-\underset{\sim}{z})\begin{bmatrix}\underset{\sim}{x}\\ \underset{\sim}{y}\\ \tilde{0}\end{bmatrix}+\underset{\sim}{z}\begin{bmatrix}\underset{\sim}{x}\\ \underset{\sim}{y}\\ \tilde{\theta}\end{bmatrix}=\begin{bmatrix}x\\ y\\ z\end{bmatrix},
\end{aligned}$$

where in the last step we have used (7). By definition, one can conclude that $\{w_i^0\}$ forms a set of generalized barycentric coordinates on the prism K.

Next, consider the case when K is a cone. Again, by $\sum_{i=1}^{n}\underset{\sim}{w}_i^0=1$ one gets

$$\sum_{i=1}^{n+1}w_i^0=\sum_{i=1}^{n}(1-\underset{\sim}{z})\pi^*\underset{\sim}{w}_i^0+\underset{\sim}{z}=(1-\underset{\sim}{z})\pi^*(1)+\underset{\sim}{z}=(1-\underset{\sim}{z})+\underset{\sim}{z}=1.$$

Denote by $(x_i,\ y_i,\ 0)$, $1\le i\le n$, the coordinates of bottom vertices. The apex has coordinates $(0,0,\theta)$. Then

$$\begin{aligned}
&\sum_{i=1}^{n}\begin{bmatrix}x_i\\ y_i\\ 0\end{bmatrix} w_i^0+\begin{bmatrix}0\\ 0\\ \theta\end{bmatrix} w_{n+1}^0=\sum_{i=1}^{n}\begin{bmatrix}x_i\\ y_i\\ 0\end{bmatrix}(1-\underset{\sim}{z})\pi^*\underset{\sim}{w}_i^0+\begin{bmatrix}0\\ 0\\ \theta\end{bmatrix}\underset{\sim}{z}\\
&\quad=(1-\underset{\sim}{z})\pi^*\left(\sum_{i=1}^{n}\begin{bmatrix}x_i\\ y_i\\ 0\end{bmatrix}\underset{\sim}{w}_i^0\right)+\begin{bmatrix}0\\ 0\\ \theta\end{bmatrix}\underset{\sim}{z}=(1-\underset{\sim}{z})\pi^*\begin{bmatrix}\underset{\sim}{x}\\ \underset{\sim}{y}\\ \tilde{0}\end{bmatrix}+\begin{bmatrix}0\\ 0\\ z\end{bmatrix}\\
&\quad=(1-\underset{\sim}{z})\begin{bmatrix}\underset{\sim}{x}\\ \underset{\sim}{y}\\ \tilde{0}\end{bmatrix}+\begin{bmatrix}0\\ 0\\ z\end{bmatrix}=\begin{bmatrix}x\\ y\\ z\end{bmatrix},
\end{aligned}$$

where in the prove we have used (9). Therefore $\{w_i^0\}$ forms a set of generalized barycentric coordinates on the cone K. □

Then we can prove the main theorem of this section:

Theorem 6.2 *On a prism/cone K, one has $\mathcal{N}^p\subset M^p(K)$, for $p=0,1,2$.*

Proof By Lemma 6.1, one immediately sees that $M^0(K)$ contains the space of all linear functions, i.e., $\mathcal{N}^0$. We just need to prove the result for $p=1,2$.

Consider the case of extrusion. Note that the extrusion formulae of Whitney forms have the same format for all kinds of base polygons, and depend linearly on $\underset{\sim}{w}_i^p$ and $\underset{\sim}{w}_i^{p-1}$. When the base polygon $\underset{\sim}{K}$ is a triangle, it is known [7] that the extrusion

produces exactly the Whitney forms corresponding to the lowest-order Nédélec–Raviart–Thomas elements on a triangular prism [27], which are known to contain $\mathcal{N}^p$. Therefore we only need to show that on a polygonal $\underset{\sim}{K}$, the space spanned by $\{\underset{\sim}{w}_i^p\}$, for $p = 0, 1, 2$ contains the corresponding space defined on a triangular $\underset{\sim}{K}$. This is indeed true by the properties of GBCs and Lemma 2.3.

Next, consider the case of conation. The conation formulae of Whitney forms w_i^p, for $p = 1, 2$, depend linearly not only on $\underset{\sim}{w}_i^p$, but also on w_i^{p-1}. Since we already have $\mathcal{N}^0 \subset M^0(K)$, the previous argument still works when combined with induction. When the base polygon $\underset{\sim}{K}$ is a triangle, the conation produces exactly $\mathcal{N}^p$, i.e., the Whitney forms on a simplex. Following the same argument as in the case of extrusion and using induction, this completes the proof of the theorem. □

Remark 6.3 By the finite element theory and Theorem 6.2, the H^1, $H(\mathrm{curl})$ and $H(\mathrm{div})$ conforming finite element spaces, defined using the vector proxy of $M^p(K)$ for $p = 0, 1, 2$, have the same order of approximation error as the lowest-order Nédélec–Raviart–Thomas finite element spaces. More specifically, on a mesh with characteristic size h, one expects that the L^2 norm approximation error of the vector proxy be of order $O(h^2)$, $O(h)$ and $O(h)$, respectively, for H^1, $H(\mathrm{curl})$ and $H(\mathrm{div})$ elements, while the L^2 norm error of the exterior derivative be of order $O(h)$ for all three cases. Indeed, for the $H(\mathrm{curl})$ ($p = 1$) and $H(\mathrm{div})$ ($p = 2$) elements, as long as $M^p(K)$ contains the space of all constants, the approximation order of the vector proxy is still the same. But the $O(h)$ approximation rate of the exterior derivative requires that $M^p(K)$ contains $\mathcal{N}^p$.

7 Numerical results

In this section we present numerical results for the H^1, $H(\mathrm{curl})$ and $H(\mathrm{div})$ conforming finite elements on prisms/cones. In all experiments, we choose the Wachspress element [30,31] as the GBC on the base polygons, and set $\boldsymbol{x}_*$ in Lemma 2.2 to be the barycenter.

We first perform numerical experiments on prism meshes. Let $\Omega = (0, 1)^3$. Divide the xy-crosssection of Ω into a centroidal Voronoi tessellation [13] with n^2 cells, and divide the z direction of Ω into n equal subintervals. This gives a quasi-uniform mesh with n^3 prisms and the prisms have polygonal bases, as shown in Fig. 3. Denote by $h = 1/n$ the characteristic mesh size. We test the interpolation errors of the H^1, $H(\mathrm{curl})$ and $H(\mathrm{div})$ conforming finite elements on prism meshes with various h, and the results are reported in Fig. 4. Also reported in Fig. 4 are the mixed finite element approximation errors, discretized using the $H(\mathrm{div})$ conforming finite element space coupled with piecewise constants for L^2. The numerical results clearly show that L^2 norms of interpolation errors and their exterior derivatives are of $O(h)$, except for the L^2 norm interpolation error of the H^1-conforming element, which is of $O(h^2)$. This agrees well with known interpolation errors of the lowest-order Nédélec–Raviart–Thomas elements [26–28], and indicates that our finite elements have optimal interpolation error. The experiment also confirms that the mixed finite element approximation rates, using the $H(div)$ conforming element, are optimal.

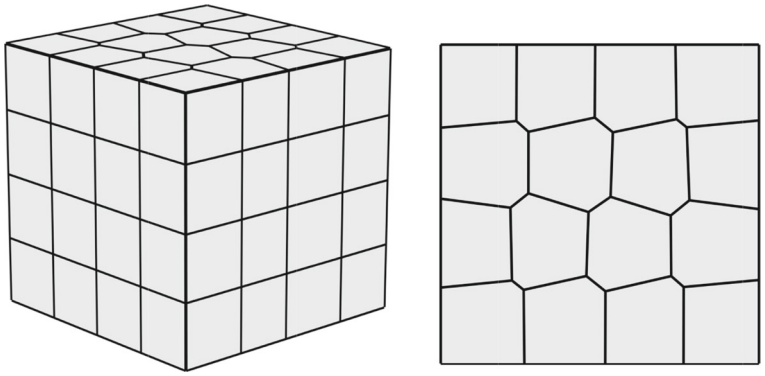

Fig. 3 A quasi-uniform prism mesh (left) and a view of its xy-crosssection (right)

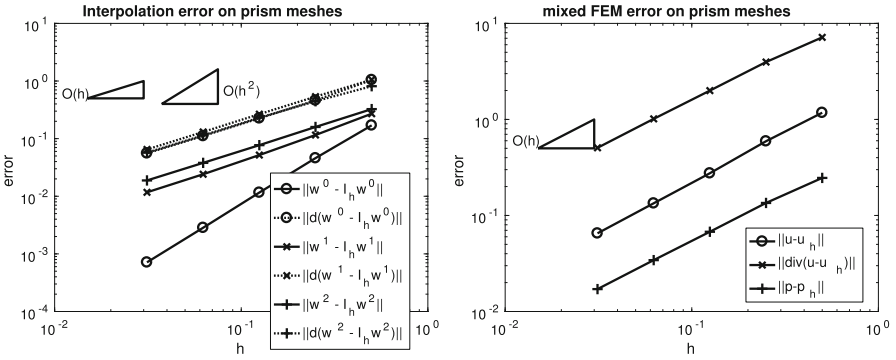

Fig. 4 Error on prism meshes with mesh sizes $h = \frac{1}{2}, \frac{1}{4}, \ldots, \frac{1}{32}$. The $\|\cdot\|$ stands for the L^2 norm in Ω. Left: interpolation errors of 0-, 1-, and 2-forms, where w^p is a p-form and I_h is its nodal value interpolation. Right: approximation error of the mixed finite element method for solving $-\Delta p = f$ in Ω, with $\boldsymbol{u} = \nabla p$ being the flux

We then test numerical results on 'quad-cone' meshes, which are generated by dividing each hexahedron in a hexahedral mesh into 6 quadrilateral-based cones, as illustrated in Fig. 5. Interpolation errors as well as the mixed finite element approximation errors are reported in Fig. 6. Again, both are optimal.

Finally, we test the interpolation error of H^1, $H(\text{curl})$ and $H(\text{div})$ conforming elements on polygon-based cones, which will be called poly-cones. For simplicity, instead of testing on a full 3D mesh, we consider randomly generated individual poly-cones, with completely random number of base-polygon vertices, random apex location, random size and position (as shown in Fig. 7). A random poly-cone is generated as follows. First, a random polygon is generated in $(0, 1) \times (0, 1)$ by computing the convex hull of 30 random points. Edges with length less than 0.1 and points with interior angle greater than 165° are removed, in order to ensure that the polygon satisfies the shape regularity conditions in [16,19]. Then, a random apex is picked in $(0, 1) \times (0, 1) \times (0.8, 1.2)$, where the range of the z-coordinate is restricted again in order to ensure shape regularity. Now the poly-cone has size $O(1)$ and can be scaled to

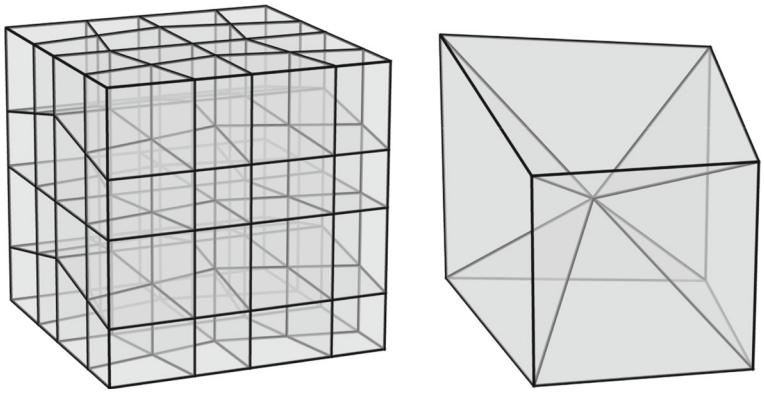

Fig. 5 A quad-cone mesh with 4^3 hexahedra (left) and each hexahedron is divided into 6 quad-cones (right)

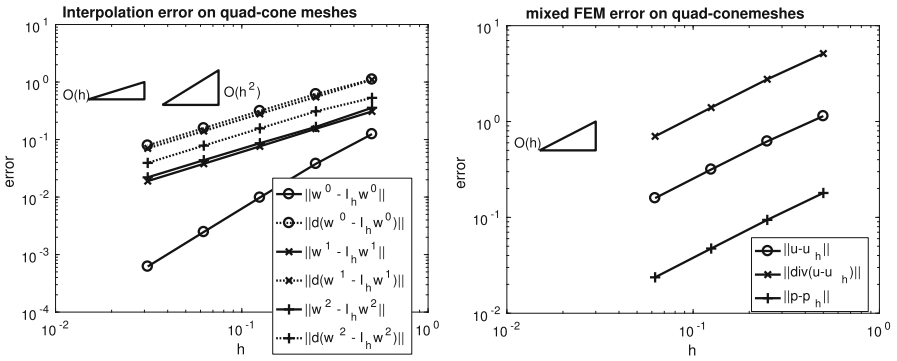

Fig. 6 Error on quad-cone meshes with mesh sizes $h = \frac{1}{2}, \frac{1}{4}, \ldots, \frac{1}{32}$. The $\|\cdot\|$ stands for the L^2 norm in Ω. Left: interpolation errors of 0-, 1-, and 2-forms, where w^p is a p-form and I_h is its nodal value interpolation. Right: approximation error of the mixed finite element method for solving $-\Delta p = f$ in Ω, with $\boldsymbol{u} = \nabla p$ being the flux

any given size h. Finally, multiply the coordinates by a random orthogonal matrix and add a random shift to the result. This rotates the poly-cone and puts it into a random position. In Fig. 8, we report the distribution of poly-cones with n-gon bases with respect to n, in two separate runs each generating hundreds of random poly-cones. It can be seen that poly-cones with hexagonal bases are of the maximum number, which is reasonable.

The numerical results are reported in Figs. 9, 10 and 11, where each circle represents the size h and interpolation error on one random poly-cone. By the standard finite element interpolation analysis, we expect an $O(h^2)$ interpolation error for the 0 form in L^2 norm, in a quasi-uniform poly-cone mesh with characteristic size h, over the entire Ω. The total number of poly-cones in the mesh is of $O(h^{-3})$. Assuming that the error is evenly distributed over the poly-cones, one expects an $O(\sqrt{(h^2)^2/h^{-3}}) = O(h^{3.5})$ interpolation error on each poly-cone. Similarly, we expect an $O(h^{2.5})$ interpolation error for the 1- and 2-forms as well as the exterior derivatives of the 0-, 1-, and 2-forms in L^2 norm. The results in Figs. 9, 10 and 11 agree well with our expectations.

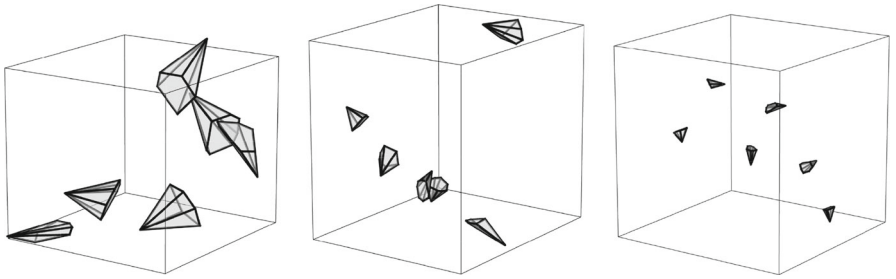

Fig. 7 Random poly-cone meshes with $h = \frac{1}{4}, \frac{1}{8}, \frac{1}{16}$

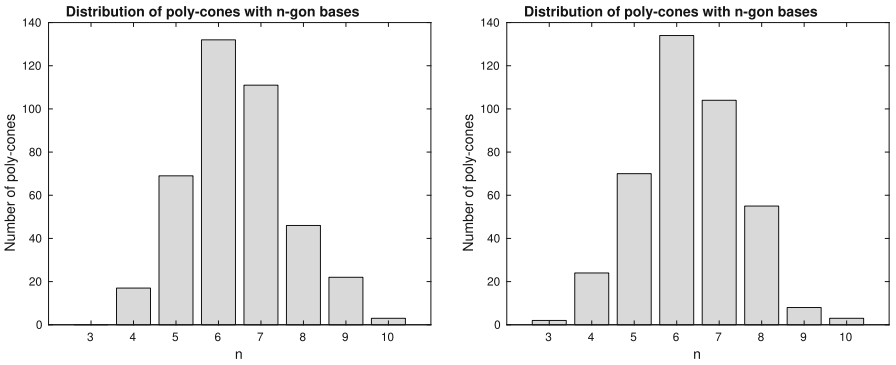

Fig. 8 Random poly-cone distribution over the number of vertices in the base polygon

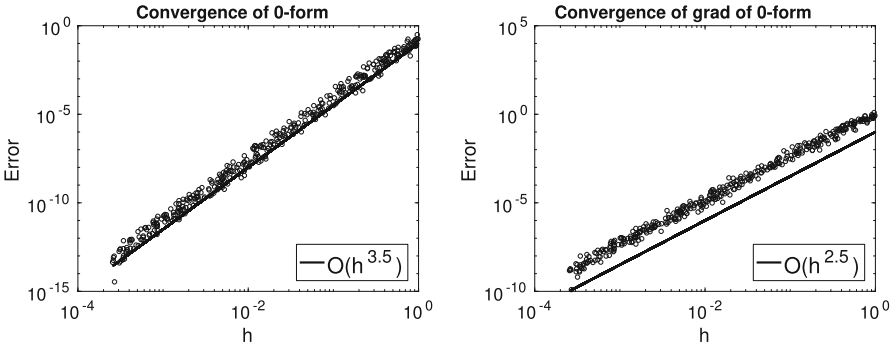

Fig. 9 Interpolation error in L^2 norm of 0-form on random polycones with various sizes

Acknowledgements Wang is supported by the Natural Science Foundation of China under grant numbers 11671210 and 91630201. Chen is supported by the Grants NSFC 11671098, 91630309, a 111 Project B08018 and Chen also thanks Institute of Scientific Computation and Financial Data Analysis, Shanghai University of Finance and Economics or support during his visit.

A Matlab code for poly-cone

We present a 100-line Matlab code for evaluating the vector proxies of Whitney 0-, 1-, and 2-forms, as well as their exterior derivatives, at given points in a poly-cone,

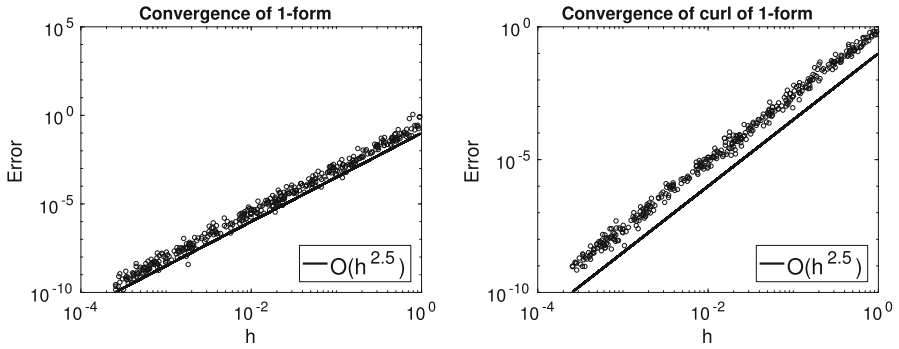

Fig. 10 Interpolation error in L^2 norm of 1-form on random polycones with various sizes

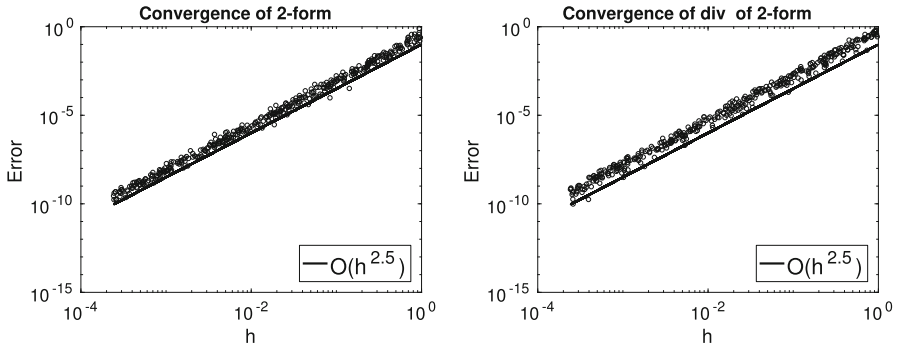

Fig. 11 Interpolation error in L^2 norm of 2-form on random polycones with various sizes

i.e., a cone with polygonal base. The code also contains a subroutine which computes vector proxies of 2D Whitney forms and their exterior derivatives on the base polygon, where the Wachspress coordinates are used to define the 0-forms. The code requires Matlab version R2016b or higher, since it uses the 'implicit expansion' feature.

The code requires that the input poly-cone must have its base on the xy-plane and apex at `[0,0,a]` where `a`$= \theta$ is the height of the poly-cone. Note that any random poly-cone can be easily converted to such one by a simple rotation and shifting. We emphasize that rotation and shifting do not alter the definition of degrees of freedom for $H(div)$ and $H(curl)$ elements. This is different from the case of a general affine transformation, in which the Piola transformation must be used to get the correct shape functions.

In the code, `[x, y, z]` stands for the coordinates of points to evaluate the Whitney forms, which are usually the Gaussian points. We do not have Gaussian quadrature on a poly-cone. However, one can easily divide the poly-cone into simplices and then use the Gaussian quadrature on sub-simplices to do numerical integration on the poly-cone. `[xs, ys, zs]` stands for $(\underset{\sim}{x}, \underset{\sim}{y}, \underset{\sim}{z})$, as defined in (9). The subroutine `baseShapes` calculates the 2D Whitney forms on the base polygon, evaluated at points `[xs, ys]`. The subroutine `pullback` computes the scaled pullback operator Π^* of 0-, 1-, and 2-forms.

```
%% Evaluate shape function of Whitney k-forms at points (x,y,z) on polycone
function [shape, dshape] = shapePolycone(k, P, x, y, z)
% The polycone must have base on xy-plane and apex at (0,0,a) with a>0.
% INPUTS: ===================================
%   k -- tells shapePolycone to compute the Whitney k-form
%   P -- 3*(n+1) matrix defining verices of poly-cone, with the first n
%        verices on the xy-plane (ordered counterclockwisely) and the
%        (n+1)th vertex (apex) at coordinate (0,0,a), with a>0.
%   x, y, z -- 1*m vectors, coordinates of points to evalute functions on
% OUTPUTS: ==================================
%   shape, dshape -- value of Whitney k-forms and exterior derivatives on
%                    points (x,y,z). Each is a 3D array where:
%   dim-1: index of Whitney k-forms, eg. 1:n+1 for 0-form, 1:2*n for 1-form
%   dim-2: index of evaluating points, i.e., 1:m
%   dim-3: dimension of vector-proxy, eg. 1:1 for 0-form, 1:3 for the
%          exterior derivative of 0-form, 1:3 for 1-form, etc.
%-------------------------------------------------------------------------
n = size(P,2)-1; % no. of vertices on base polygon
m = size(x,2);   % no. of evaluating points
a = P(3, n+1);   % height of poly-cone
zs = z/a;       xs = x./(1-zs);     ys = y./(1-zs);  % projected coordinate
[shape0B,dshape0B,shape1B,dshape1B,shape2B] = baseShapes(P(1:2,1:n),xs,ys);
%------------------------------------------------------------ compute 0-form
shape0 = [(1-zs).*shape0B; zs];
dshape0(1:n+1,1:m,3) = 1/a * [-shape0B; ones(1,m)];
dshape0(1:n,:,:) = dshape0(1:n,:,:) + pullback(1, dshape0B, a, xs, ys);
if k>0 %------------------------------------------------- compute 1-form
dzs(1:n,1:m,3) = 1/a;  % d(zs) is a 1-form
shape1(n+1:2*n,1:m,1:3) = zs.*dshape0(1:n,:,:) - shape0(1:n,:).*dzs;
shape1(1:n,:,:) = (1-zs) .* pullback(1,shape1B,a,xs,ys);
dshape1(n+1:2*n,1:m,1:3) = 2 * cross(dzs,dshape0(1:n,:,:),3);
dshape1(1:n,:,:) = 2/a*cat(3,shape1B(:,:,2),-shape1B(:,:,1),zeros(n,m)) ...
                   + pullback(2,dshape1B,a,xs,ys);  end
if k>1 %------------------------------------------------------ compute 2-form
shape2(2:n+1,1:m,1:3)=zs.*dshape1(1:n,:,:)-2*cross(dzs,shape1(1:n,:,:),3);
shape2(1,:,:) = (1-zs) .* pullback(2,shape2B,a,xs,ys);
dshape2 = [-3/a * shape2B; 3 * dot(dzs, dshape1(1:n,:,:),3)]; end
%------------------------------------------------------------ return k-form
shape = eval(['shape', int2str(k)]); dshape = eval(['dshape', int2str(k)]);
end

%% Evaluate shape function of Whitney 0,1-forms at points (x,y) on polygon.
function [shape0, dshape0, shape1, dshape1, shape2] = baseShapes(v, x, y)
% Wachspress generalized barycentric coordinates are used in computation.
% INPUTS: ===================================
%   v -- 2*n matrix defining verices of polygon, ordered countclockwisely
%   x, y -- 1*m vectors, coordinates of points to evalute functions on
% OUTPUTS: ==================================
%   shape(*), dshape(*) -- value of Whitney *-forms and their exterior
%      derivatives on points (x,y). See FUNCTION shapePolycone for details.
%-------------------------------------------------------------------------
n = size(v,2);    m = size(x,2);  % no. vertices and no. evaluating points
[un, edgeL] = getNormals(v);      % unit outward normal and edge length
area = polyarea(v(1,:), v(2,:));  % area
centroid = getCentroid(v, area);  % centroid
vc = [v, v(:,1)] - centroid;      %---- K contains area of subtriangles K_i
K = 0.5*( vc(1,1:n).*vc(2,2:n+1) - vc(2,1:n).*vc(1,2:n+1) );
%------------------------------------------------------------ Define coefficients
% See "Minimal degree H(curl) And H(div) conforming finite elements on
% polytopal meshes" by W.Chen and Y.Wang, Math. Comp. (2017) for details.
B = diag(edgeL) - edgeL'*K / area;      B = [B, B];     C = zeros(n,n);
for j=1:n, C(:,j) = -1/n * sum( (1:(n-1)) .* B(:,(j+1):(j+n-1)), 2 ); end
%------------------------------------------ Define intermediate variables
% See "Generalized barycentric coordinates and applications", M. S. Floater
%      in  Acta Numerica, (2015) for details.
% h -- n*m mat,   h(i,j) is the distance from [x(j),y(j)] to the ith edge
% p -- n*m*2 mat, P(i,j) = un(i) / h(i,j)
% w -- n*m mat,   w(i,j) = (un_{i-1} x un_i) / h(i-1,j) / h(i,j)
% R -- n*m*2 mat, R(i,j) = p(i-1,j) + p(i,j)
h = (v(1,:)'-x).*un(1,:)' + (v(2,:)'-y).*un(2,:)';
p = cat(3, un(1,:)' ./h, un(2,:)' ./h);
im1 = [n,1:n-1];  % the (i-1) index for i from 1 to n
w = (un(1,im1).*un(2,:)-un(2,im1).*un(1,:))' ./ ( h(im1,:) .* h );
R = p(im1, :,:) + p;
%------------------------------------------------- Define shape functions
shape0 = w ./ sum(w,1);         dshape0 = shape0 .* (R - sum(shape0.*R,1));
shape1(:,:,2) = 0.5/area *(x-centroid(1,:)) - (C*dshape0(:,:,2)) ./edgeL';
shape1(:,:,1) = 0.5/area *(centroid(2,:)-y) - (C*dshape0(:,:,1)) ./edgeL';
dshape1 = repmat(1/area,n,m);                  shape2 = repmat(1/area,1,m);
end

%% Compute scaled-pullback of k-form from base polygon to the polycone.
function [pw] = pullback(k, w, a, xs, ys)
% Compute pw = (1-zs)^k * (Pi^* w), evaluated on points (xs, ys, zs). Here
% a is the poly-cone height. Input w must have size n*m*2 for 1-form and
% n*m for 0,2-form. Output pw has size n*m for 0-form, n*m*3 for 1,2-form.
switch k
  case 0, pw=w;
  case 1, pw=cat( 3, w(:,:,1), w(:,:,2), 1/a*(w(:,:,1).*xs+w(:,:,2).*ys) );
  case 2, pw=cat( 3, -w.*xs/a, -w.*ys/a, w );
end;  end

%% Utility
function [un, edgeL] = getNormals(v) %------ polygon normal and edge length
un = diff([v,v(:,1)],1,2);      edgeL = sqrt(sum(un.^2,1));
un = [un(2,:); -un(1,:)]./edgeL;  end

function [centroid] = getCentroid(v, area) %-------------- polygon centroid
vs = [v(:, 2:end), v(:,1)];     temp = v(1,:).*vs(2,:) - v(2,:).*vs(1,:);
centroid = 1/6/area * sum((v+vs).*temp, 2);  end
```

References

1. Abraham, R., Marsden, J.E., Ratiu, T.: Manifolds, Tensor Analysis, and Applications. Springer, New York (1988)
2. Arnold, D.N., Falk, R.S., Winther, R.: Finite element exterior calculus, homological techniques, and applications. Acta Numer. **15**, 1–155 (2006)
3. Basic principles of virtual element methods: Beirão da Veiga, L., Brezzi, F., Cangiani, A., Manzini, G., Marini, L.D., Russo, A. Math. Model. Methods Appl. Sci. **23**, 199–214 (2013)
4. Bonelle, J., Di Pietro, D., Ern, A.: Low-order reconstruction operators on polyhedral meshes: application to compatible discrete operator schemes. Comput. Aided Geom. D **35**(36), 27–41 (2015)
5. Bossavit, A.: Mixed finite elements and the complex of Whitney forms. In: Whiteman, J. (ed.) The Mathematics of Finite Elements and Applications VI, pp. 137–144. Academic Press, London (1988)
6. Bossavit, A.: Whitney forms: a class of finite elements for three-dimensional computations in electromagnetism. IEEE Proc. **135**, 493–500 (1988)
7. Bossavit, A.: A uniform rational for Whitney forms on various supporting shapes. Math. Comput. Simul. **80**, 1567–1577 (2010)
8. Chen, W., Wang, Y.: Minimal degree $H(curl)$ and $H(div)$ conforming finite elements on polytopal meshes. Math. Comp. **307**, 2053–2087 (2017)
9. Christiansen, S.: A construction of spaces of compatible differential forms on cellular complexes. Math. Models Methods Appl. Sci. **18**, 739–757 (2008)
10. Di Pietro, D.A., Ern, A., Lemaire, S.: An arbitrary-order and compact-stencil discretization of diffusion on general meshes based on local reconstruction operators. Comput. Methods Appl. Math. **14**, 461–472 (2014)
11. Di Pietro, D.A., Ern, A.: A hybrid high-order locking-free method for linear elasticity on general meshes. Comput. Methods Appl. Mech. Eng. **283**, 1–21 (2015)
12. Di Pietro, D.A., Ern, A.: Arbitrary-order mixed methods for heterogeneous anisotropic diffusion on general meshes. IMA J. Numer. Anal. **37**, 40–63 (2017)
13. Du, Q., Faber, V., Gunzburger, M.: Centroidal voronoi tessellations: applications and algorithms. SIAM Rev. **41**, 637–676 (1999)
14. Floater, M.S.: Mean value coordinates. Comput. Aided Geom. Des. **20**, 19–27 (2003)
15. Floater, M.S.: Generalized barycentric coordinates and applications. Acta Numer. **24**, 161–214 (2015)
16. Floater, M., Gillette, A., Sukumar, N.: Gradient bounds for Wachspress coordinates on polytopes. SIAM J. Numer. Anal. **52**, 515–532 (2014)
17. Floater, M.S., Kós, G., Reimers, M.: Mean value coordinates in 3D. Comput. Aided Geom. Des. **22**, 623–631 (2005)
18. Frankel, T.: The Geometry of Physics: An Introduction, 2nd edn. Cambridge University Press, New York (2004)
19. Gillette, A., Rand, A., Bajaj, C.: Error estimates for generalized barycentric interpolation. Adv. Comput. Math. **37**, 417–439 (2012)
20. Gillette, A., Rand, A., Bajaj, C.: Construction of scalar and vector finite element families on polygonal and polyhedral meshes. Comput. Methods Appl. Math. **16**, 667–683 (2016)
21. Grădinaru, V.: Whitney elements on sparse grids. Dissertation, Universität Tübingen (2002)
22. Grădinaru, V., Hiptmair, R.: Whitney elements on pyramids. ETNA **8**, 154–168 (1999)
23. Hiptmair, R.: Canonical construction of finite elements. Math. Comput. **68**, 1325–1346 (1999)
24. Hirani, A.: Discrete Exterior Calculus. Ph.D. Thesis, CalTech (2003)
25. Joshi, P., Meyer, M., DeRose, T., Green, B., Sanocki, T.: Harmonic coordinates for character articulation. ACM Trans. Graph. **26**, Article 71 (2007)
26. Nédélec, J.C.: Mixed finite element in $\mathbb{R}^3$. Numer. Math. **35**, 315–341 (1980)
27. Nédélec, J.C.: A new family of mixed finite elements in $\mathbb{R}^3$. Numer. Math. **50**, 57–81 (1986)
28. Raviart, P., Thomas, J.: A Mixed Finite Element Method for Second Order Elliptic Problems. Springer Lecture Notes in Mathematics, vol. 606, pp. 292–315. Springer, New York (1977)
29. Sibon, R.: A vector identity for the Dirichlet tessellation. Math. Proc. Camb. Philos. Soc. **87**, 151–155 (1980)
30. Wachspress, E.L.: A Rational Finite Element Basis. Academic Press, Cambridge (1975)
31. Wachspress, E.L.: Barycentric coordinates for polytopes. Comput. Aided Geom. Des. **61**, 3319–3321 (2011)

32. Wang, J., Ye, X.: A weak Galerkin finite element method for second-order elliptic problems. J. Comput. Appl. Math. **241**, 103–115 (2013)
33. Wang, J., Ye, X.: A weak Galerkin mixed finite element method for second-order elliptic problems. Math. Comput. **83**, 2101–2126 (2014)
34. Warren, J.: Barycentric coordinates for convex polytopes. Adv. Comput. Math. **6**, 97–108 (1996)
35. Whitney, H.: Geometric Integration Theory. Princeton University Press, Princeton (1957)

Publisher's Note Springer Nature remains neutral with regard to jurisdictional claims in published maps and institutional affiliations.